Review Article

Applications of Metaheuristic Algorithms in Solar Air Heater Optimization: A Review of Recent Trends and Future Prospects

Jean De Dieu Niyonteze [ID],[1] **Fumin Zou,**[1,2,3] **Godwin Norense Osarumwense Asemota** [ID],[4] **Walter Nsengiyumva** [ID],[5] **Noel Hagumimana** [ID],[1] **Longyun Huang,**[1] **Aphrodis Nduwamungu** [ID],[4] **and Samuel Bimenyimana** [ID][6,7]

[1]*Fujian Key Laboratory of Automotive Electronics and Electric Drive, Fujian University of Technology, Fuzhou 350118, China*
[2]*Sub-laboratory for Southeast Asian of BDS/GNSS Open Laboratory, Fuzhou 350118, China*
[3]*National Demonstration Center for Experimental Electronic Information and Electrical Technology Education, Fuzhou 350118, China*
[4]*African Centre of Excellence in Energy for Sustainable Development, University of Rwanda, Kigali, Rwanda*
[5]*Laboratory of Optics, Terahertz and Non-destructive Testing, School of Mechanical Engineering and Automation, Fuzhou University, Fuzhou 350116, China*
[6]*Intelligence and Automation in Construction Provincial Higher–Educational Engineering Research Centre, Huaqiao University, 361021 Xiamen, China*
[7]*Hello Renewables Ltd., Kigali, Rwanda*

Correspondence should be addressed to Jean De Dieu Niyonteze; niyontezejado@gmail.com

A transition to solar energy systems is considered one of the most important alternatives to conventional fossil fuels. Until recently, solar air heaters (SAHs) were among the other solar energy systems that have been widely used in various households and industrial applications. However, the recent literature reveals that efficiencies of SAHs are still low. Some metaheuristic algorithms have been used to enhance the efficiencies of these SAH systems. In the paper, we do not only discuss the techniques used to enhance the performance of SAHs, but we also reviewed a majority of published papers on the applications of SAH optimization. The metaheuristic algorithms include simulated annealing (SA), particle swarm optimization (PSO), genetic algorithm (GA), artificial bee colony (ABC), teaching-learning-based optimization (TLBO), and elitist teaching-learning-based optimization (ETLBO). For this research, it should be noted that this study is mostly based on the literature published in the last ten years in good energy top journals. Therefore, this paper clearly shows that the use of all six proposed metaheuristic algorithms results in significant efficiency improvements through the selection of the optimal design set and operating parameters for SAHs. Based on the past literature and on the outcomes of this paper, ETLBO is unquestionably more competitive than ABC, GA, PSO, SA, and TLBO for the optimization of SAHs for the same considered problem. Finally, based on the covered six state-of-the-art metaheuristic techniques, some perspectives and recommendations for the future outlook of SAH optimization are proposed. This paper is the first-ever attempt to present the current developments to a large audience on the applications of metaheuristic methods in SAH optimization. Thus, researchers can use this paper for further research and for the advancement of the proposed and other recommended algorithms to generate the best performance for the various SAHs.

1. Introduction

World energy consumption is increasing rapidly due to population growth and technological advancements. It is essential to focus on a dependable, cost-reflective, environmentally friendly, and any naturally occurring inexhaustible source of energy for future energy requirements. Solar power is the most promising origin of clean power

[1–4]. Therefore, the exploitation and use of solar power will be pivotal to future energy development because it acts as one of the most mature and promising options [5, 6].

Solar energy systems are not greenhouse gas or pollution producers. Solar energy has a positive and indirect effect on the environment when it replaces or reduces other sources of energy usage [7–13]. However, solar energy practical applications still face major obstacles. In particular, solar air heaters (SAHs) do not only have problems related to corrosion, salt deposits, and freezing and boiling point temperatures; but they also have low thermal performance and very small heat storage capability [14–16]. Hence, the thermal performance of SAHs can be enhanced by the collector shape and design modification [16], the use of heat storage materials [17], the effect of artificial roughness [18], and other factors. Moreover, different optimization techniques such as metaheuristic algorithms have been extensively utilized to obtain sets of optimized parameter values that contribute to the thermal effectiveness of such solar heaters.

In 2014, the authors in [19] introduced an optimized SAH design having the offset strip fin absorber plate using a numerical model. A comprehensive analysis of the heater's thermal effectiveness was determined using the American Society of Heating, Refrigerating and Air-Conditioning Engineers (ASHRAE) Standard 93-2003 to measure the time constant, thermal efficiency, incident angle modifier, and synthetic resistance coefficient. The results showed that their research would be helpful in developing energy-efficient and cost-effective SAHs. In the same year, a study by Kumar and Kim [20] successfully obtained effective thermal efficiencies of a SAH duct on the heated plate using different types of roughness geometries. The roughened discrete multiple V-shaped ribbed SAHs have better thermal efficiencies than the transverse, angled, discrete, multiple, and W-rib roughness-shaped SAHs.

Some other researchers developed optimization methodologies based on genetic algorithm (GA), particle swarm optimization (PSO), artificial bee colony (ABC), simulated annealing (SA), and teaching-learning-based optimization (TLBO). The GA was used in [21] to find optimal parameters in flat plate SAHs with ribbed surfaces. The authors found that under low air mass flow conditions, using ribs in a flat plate SAH improved thermal efficiency by more than 9%. Elsheikh and Abd Elaziz [22] reviewed the components of solar energy system applications of PSO to include solar collectors, solar cells, solar power towers, photovoltaic/thermal systems, and solar stills. The study indicated that the PSO is a likely technique to improve the efficiency of solar energy systems. A recent study by Yıldırım and Aydoğdu [23] optimized flat plate SAHs including single-pass SAH and double-parallel pass SAH using ABC algorithm. The authors in this study obtained the operating values and optimum design using the ABC algorithm with different insolation values and collector lengths. Interestingly, a study by Rao and Waghmare [24] used the effectiveness of the TLBO technique to secure the optimal design and operating parameters for a smooth flat plate SAH. Furthermore, the TLBO results are similar to other metaheuristic algorithms like SA, PSO, and GA.

In summary, this paper mainly undertakes a detailed review of six metaheuristic algorithms in solar air heater optimization. This comprehensive literature research is conducted as a source of knowledge and validation complemented by a systematic review of the modeling, performance enhancement techniques, and optimization of these systems. Some works related to the application of metaheuristic algorithms in solar systems were reported earlier, for instance, the use of these techniques in PV parameter estimation, identification, and extraction problems [25–29]. However, this paper is the first-ever attempt to present the recent trends on the applications of metaheuristic techniques in SAH optimization to a wide audience. It is undoubtedly believed that the information outlined in this paper will guide researchers in the innovative SAHs and performance enhancement for the current heaters.

As shown in Figure 1 below, the rest of the paper is organized as follows: the research methodology is in Section 2; a historical survey, classification, application, and performance of SAHs are presented in Section 3. Section 4 gives the metaheuristic algorithms for SAH optimization, while a comprehensive discussion, conclusions, and future outlook are provided in Sections 5 and 6.

2. Research Methodology

An instruction to explore appropriate papers in SAHs (history, classification, application, and performance) and SAH optimization is described in this section. Our survey is logical, appropriate, specific, applicable, and searchable due to the method used to probe and obtain knowledge-rich data.

2.1. Filter Keyword Searches. When searching scientific electronic databases, the use of the most appropriate keywords plays a vital role in extracting from scientific databases the most suitable research papers in a specific area of study. In this study, we used the following main keywords to obtain the relevant results for solar air heaters, metaheuristic algorithms, and optimization. Furthermore, the following giant academic publishers were used to initialize our search process: IEEE Xplore, Elsevier, John Wiley & Sons, ACM Digital Library, Taylor & Francis, Springer, and Hindawi.

2.2. Question Formulations. As mentioned above, the objective of this survey paper is to explore and consider all the studies that have been conducted on solar air heater optimization using metaheuristic algorithms. Hence, the following research questions were considered in the study:

Question 1. Which optimization algorithms have been conducted as a framework for SAH optimization?

Question 2. What is the performance of the optimization of SAH algorithms?

Question 3. What are the advantages, disadvantages, and limitations of each algorithm?

Question 4. What are the research trends and future prospects?

Certainly, Sections 5 and 6 of this paper clearly elaborate more on all the above research questions.
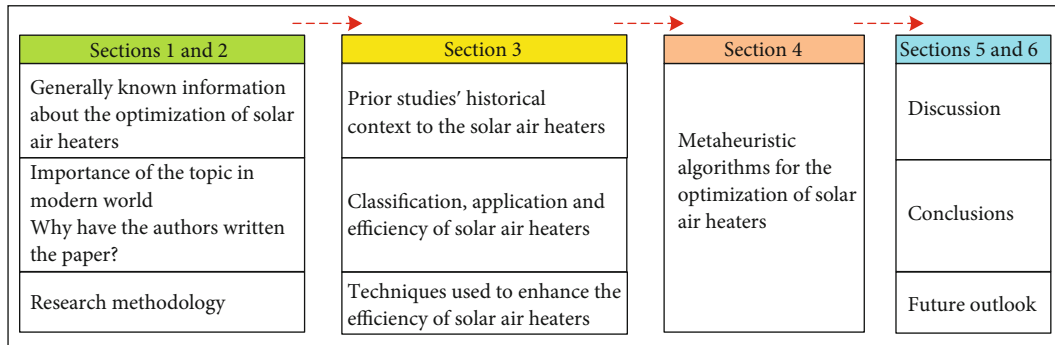
Sections 1 and 2	Section 3	Section 4	Sections 5 and 6
Generally known information about the optimization of solar air heaters	Prior studies' historical context to the solar air heaters	Metaheuristic algorithms for the optimization of solar air heaters	Discussion
Importance of the topic in modern world	Classification, application and efficiency of solar air heaters		Conclusions
Why have the authors written the paper?			
Research methodology	Techniques used to enhance the efficiency of solar air heaters		Future outlook

FIGURE 1: Roadmap of this paper.

2.3. Exploring Data and Paper Selection. The appropriate research papers of SAH optimization were explored in academic databases, resulting in the subject categorizations of the topic. In the exploration process, the principles used are summarized below:

(1) Published research papers in the last ten years

(2) Published research papers on SAHs

(3) Published research papers on SAH optimization

(4) Published research papers on SAH optimization using metaheuristic algorithms

Our search survey attempted to gather and review almost all the work carried out in the area of optimization of SAHs and to filter out those inappropriate academic papers. We therefore used 224 published papers (references) for further research investigation and analysis, mostly between 2010 and 2020. More importantly, this survey showed that there is no other review paper that presents the recent trends on the applications and future prospects of metaheuristic techniques in SAH optimization.

Although there are not many research papers on the optimization of SAHs using the metaheuristic algorithms, this survey has shown that the total number of publications on this topic has increased slightly since 2010. Fortunately, the metaheuristic algorithms like the artificial bee colony (ABC), genetic algorithm (GA), particle swarm optimization (PSO), simulated annealing (SA), and teaching-learning-based optimization (TLBO) were used in this survey. It is therefore clear that the use of various promising metaheuristic algorithms to optimize SAHs has clarified the scope for further improvements. Figure 2 below graphically illustrates the list of metaheuristic algorithms based on the work of authors in Ref. [26]. This provides a better view and understanding of those algorithms that have been applied and not yet applied in SAH optimization.

3. Solar Air Heaters

3.1. A Historical Overview of the Solar Air Heaters. The technology of solar air heating has been in use for many years, especially for heating the ventilation air. Daniels et al. [30] first used solar heat-stored iron in 1877. Four years later, E

Morse (an American) designed and produced the first accredited SAH [31, 32]. The first SAH system was an uncomplicated wooden wall-hung cabinet of a black sheet of metal covered with transparent glass that is called a solar collector today. The function of the SAH system was purely based on convection, in which the hot air is emitted through the solar-heated steel plate inside the system panel. Also, the hot air is primarily replaced with the cool air entering the building at the foot of the cabinet. However, the system brought scant attention, even though modifications appeared. It is not well known if any of these SAH types were factory produced [31, 32].

In the nineteen-twenties, the term solar house was firstly written in the United States newspapers to express how their large south-facing windows absorb the heat from the sun directly [33]. Later on, solar houses ("House of Tomorrow and Crystal House at the Chicago World Fair") were pioneered by G & W Keck (architects) in 1932 and 1933, respectively. In summer, they used featured overhangs to shade against overheating. On sunny winter days, interior masonry walls and floors were used to absorb the heat for later release in the cooler evenings (this principle is called "thermal mass" today) [33]. The year 1938 denotes the inception of modern research into solar heating at the Massachusetts Institute of Technology by Godfrey L. Cabot, according to a study by Duffie and Beckman [34]. Consequently, the program led to the development of methods in collector performance calculations, in which some changes or improvements are the standard methods in use today. A series of six solar-heated structures were also successfully developed as a result of the program. Furthermore, a residence called the "MIT House IV" was a well-furnished, meticulously designed, and effectively orchestrated solar water heater (SWH) and water storage system.

Then, other significant developments in SAHs came during the 1940s [33]. In this situation, K Miller (an American) patented a system that used solar collectors to heat air and then pumped it into a granulated rock-filled storage container. This invention benefited from the heat stored by the rock that could be released later at night when the exterior air temperature became too cool. This arrangement was a dependable ancillary heat source that balances a portion of the energy consumption in households, which was also automated with thermostats, and fans. Later on, a new application with solar air heating was explored by two residences in

Biology-based algorithms	References
(i) Genetic algorithm	[203], [202], [159], [204]
(ii) Differential evolution	
(iii) Artificial bee swarm optimization	
(iv) Artificial bee colony	[203], [23]
(v) Whale optimization algorithm	
(vi) Improved ant lion optimizer	
(vii) Biogeography based optimization	
(viii) Cuckoo search	
(ix) Bird mating optimization	
(x) Flower pollination algorithm	
(xi) Grey wolf optimization	
(xii) Bacterial foraging algorithm	
(xiii) Artificial immune system	
(xiv) Salp swarm algorithm	

Sociology-based algorithms

References
[200], [24], [84]

(i) Harmony search algorithm
(ii) Teaching learning based optimization
(iii) Imperialist competitive algorithm
(iv) Multiple learning backtracking search algorithm

Meta-heuristic algorithms

Mathematics-based algorithms

References

(i) Pattern search algorithm
(ii) Shuffled complex evolution
(iii) JAYA algorithm

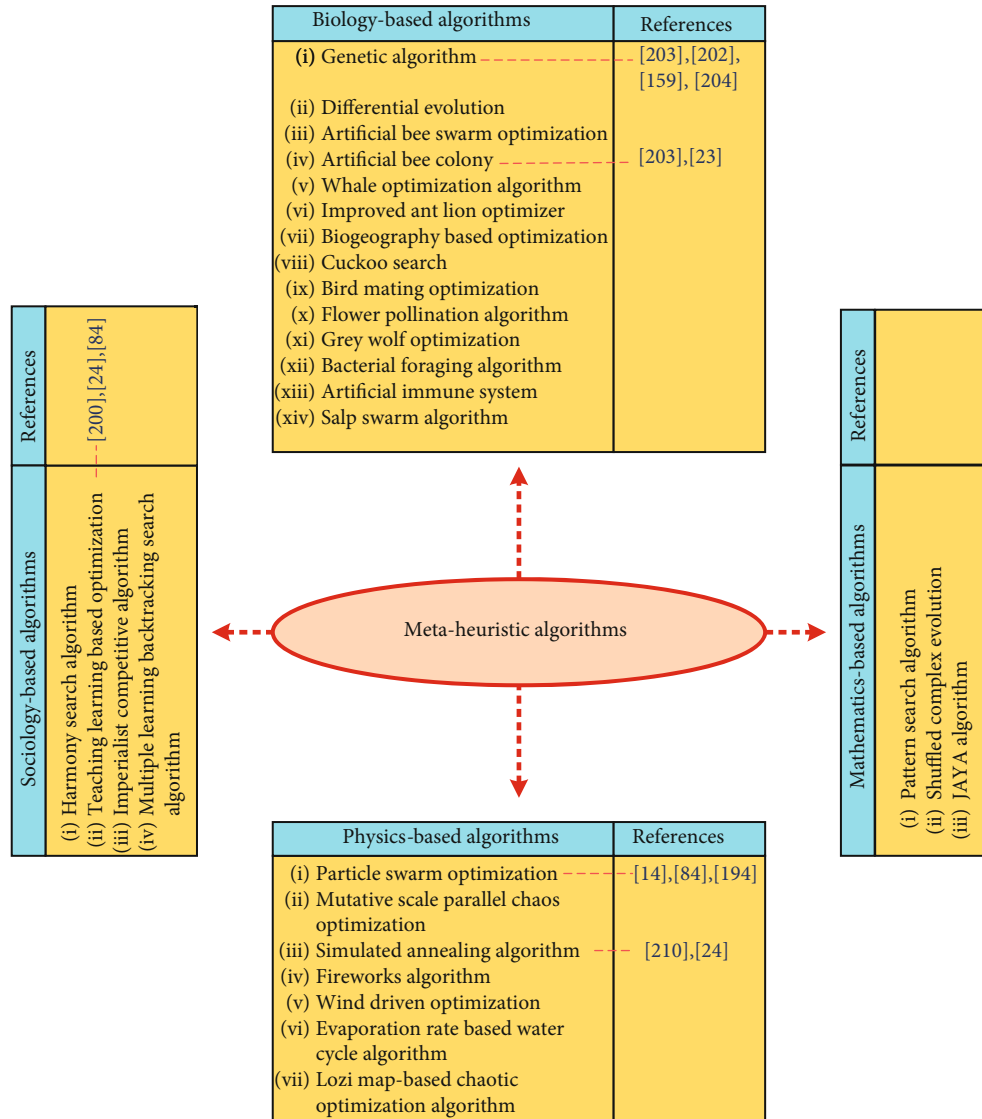| Physics-based algorithms	References
(i) Particle swarm optimization	[14], [84], [194]
(ii) Mutative scale parallel chaos optimization	
(iii) Simulated annealing algorithm	[210], [24]
(iv) Fireworks algorithm	
(v) Wind driven optimization	
(vi) Evaporation rate based water cycle algorithm	
(vii) Lozi map-based chaotic optimization algorithm	

Figure 2: Classification of metaheuristic algorithms (biology-based algorithms, physics-based algorithms, sociology-based algorithms, and mathematics-based algorithms) and their applications in SAH optimization. Note: some algorithms do not have any references (that means they have never been applied to SAH optimization yet).

Massachusetts between 1946 and 1949 [32, 33]. The new system application used solid chemical compounds to absorb energy and subsequently release the heat by fusion when transformed from the solid state into the liquid state. This phase change material (PCM) technology has many applications in the industry.

From the 1940s to the 1950s, several Americans made innovations to the previous solar collector design to further substantiate their true potentials [33]. By 1955, Bliss [32, 34, 35] developed and evaluated the efficiency of a 100% Arizona desert solar-heated house in the US. In the design, a flow-through air heater matrix and thermal energy storage (TES) system were used. Although the as-built system did not indicate an economic optimum, a smaller system using some other ancillary energy sources resulted in a lower optimum cost. In 1959, a new air heating system used the Lof design with transparent glass plate collectors and a TES pebble bed. Hence, Lof used these concepts to construct a home

near Denver, Colorado, which he and his family lived since 1959. During the first years of its operation, the system effectiveness was studied and described by Lof et al. in two phases, (1963, 1964) and (1976 to 1978) [32, 34]. Their system efficiency in the second assessment period was approximately 78.0% of the original model. This system provided proof of robust and well-arranged air systems able to operate for many years with little maintenance [34].

In 1968, Close et al. [32, 34] described how another type of SAH partially heated a laboratory building in Australia. The system was a $56.0 \, m^2$ vee-grooved SAH that incorporated pebble bed storage. The established 55.0°C air outlet temperature occurred because the inflected airflow passed through the collectors. Many different types of air heating systems have been experimentally constructed, and the performance of some has been evaluated and reported since 1970. Lastly, in 2003, Weiss et al. [36] comprehensively studied the optimization designs of assorted European "solar

combisystems" (a solar house comprising space heating, cooling, and hot water systems). Table 1 particularly summarizes the highlights of the important dates in the history of the invention and development of SAHs and the important historical advances made in the first periods of the development of SAH technology.

3.2. Distribution of Solar Air Heaters.
SAHs can be arranged according to a study by Ghritlahre et al. [37]. This study indicates that SAHs can be categorized according to the collector cover (glass), absorber materials, absorbing surface shape, absorber flow pattern, flow types, hybrid collectors, and applications. Each major SAH group is subdivided into subgroups, as illustrated in Figure 3 below.

3.3. Utilization of Solar Air Heaters.
Every hour, the earth receives more heat energy from the sun than the entire world uses in a year. Also, solar energy systems for houses are increasing in popularity, especially because installation prices are decreasing, generally [38–43]. Solar air heating is another renewable energy technology, which potentially promises climate change mitigation, future sustainable energy for all, and global economic benefits as well. SAHs have been widely used in different parts of the world for many applications. Basically, solar heating systems are used in drying, preheating, space cooling, and heating [37], as shown in Figure 3 and in the previous subsection.

3.3.1. Drying Agricultural Produce.
Drying agricultural produce involves a lot of effort, but previous research shows that enhancing energy efficiency by only 1.0% could boost profits by 10.0% [44]. Back in 2017, the literature has shown that researchers tremendously studied numerous SAHs that can be operated for crop drying applications. Recent research by Tomar et al. [45] used the thermophysics of crops, systems, and components to study solar dryers applied to tropical food preservation. On the whole, the study shows that solar crop drying stems from crop decay and causes us to better understand the complexities and the interrelationships between internal crop structures, human nourishment, and food aesthetics. Furthermore, research studies that condense the universal crop, dryer, and climate change nexus were recommended in future analyses.

In 2017, Shamekhi-Amiri et al. [46] constructed an indirect mode solar dryer system of lemon balm leaves and the thermal performance was then experimentally investigated under a certain case study. The results indicate that increasing the flow rate from $0.006125 \, m^3/s$ to $0.01734 \, m^3/s$ upgraded the thermal efficiency of the collector by nearly 20.0%. Two years later, the thermal performance analysis of a quadruple-pass solar air collector- (QPSAC-) assisted pilot-scale greenhouse dryer was successfully conducted [47]. In this experiment, red pepper and kiwi were dried as products in the constructed drying system. Interestingly, they used the performance tests at 0.008 and 0.010 kg/s flow rates, respectively, and the mean thermal efficiency for QPSAC was between 71.63 and 80.66%. Moreover, the temperature of 28.10°C at the 0.008 kg/s airflow rate was the highest instantaneous temperature difference in the QPSAC system.

3.3.2. Solar Air Preheating.
Obviously, using solar thermal energy for heat has a lot of potentials. Efficient systems are currently available, require very little maintenance, and generate energy savings. Over recent years, photovoltaic/thermal (PV/T) hybrid systems, which basically transform solar energy into electricity and heat, respectively, are the most recommended promising air systems for future air preheating applications [48–50]. However, some improvements can still be made to enhance the maintenance cost, efficiency, and effectiveness of PV/Ts.

In this case, studies [48, 51–53] exceptionally highlighted using new innovative technologies like nanofluids and PCM that could ultimately increase the PV/T's system performance.

From 2017, extensive studies have proposed and evaluated the thermal behavior of solar air preheating systems. For instance, studies [54–56] experimentally developed various air preheating systems that can highly increase thermal efficiency. On the whole, they have all noted that solar air preheating systems could successfully improve the energy efficiency of buildings, which definitely reduce energy bills and greenhouse gas emissions.

3.3.3. Solar Space Heating.
Until recently, solar space heating technology has seen major improvements. These systems use safety technology to reduce fossil fuel use, which leads to a reduction in carbon footprint. In 2015, Tyfour et al. [57] designed and tested a simple islanded hot air space heating system to work in parallel with any other conventional space heating systems. Various arrangements of multipanel installations have been constructed and tested, and the results indicate that in a multipanel installation, the vertical expansion gives higher system efficiency. In 2017, a dark solar air collector (SAC) with a punctured absorber plate was theoretically and empirically studied in western Iraq, which compared both the economic characteristic and thermal performance with other heating systems [58]. The study concluded that this SAC is superior in economic and thermal performance during clear and cloudy winter days under western Iraq climatic conditions.

By 2019, a space heating solar air source heat pump and domestic hot water system were proposed and numerically modeled in three places within China (Chengdu, Beijing, and Shenyang) [59]. The results showed that the solar air source heat pump mode provided the heat which was between 11.0% and 15.0% of the total heat production in these three places. This also indicates that weak solar radiation can be harnessed. Secondly, in terms of defrosting conditions, the results indicate that the systems proved to have a large energy saving potential. Finally, the seasonal performance factor was 3.61, 3.27, and 2.45 in Chengdu, Beijing, and Shenyang, respectively, during summer, and the energy saving rate ranged between 9.0% and 52.0% when compared with the traditional air source heat pump system.

3.3.4. Solar Air Conditioning.
Researchers have talked about solar air conditioning systems for years. The study by Nkwetta and Sandercock [60] indicates that solar air conditioning (solar cooling) is a good and more environmentally

TABLE 1: Important dates in the history of the invention and development of solar air heaters.

| S. no.	Decade	Year	Description of the system/invention/research	Researcher/inventor/reporter	References
1.	1870s	1877	The first-ever used solar heat-stored iron.	Daniels et al.	[30]
2.	1880s	1881	The first-ever designed accredited solar air heater. It was an uncomplicated wooden wall-hung cabinet of a black sheet of metal covered with transparent glass.	E Morse	[31, 32]
3.	1920s	—	The phrase "solar house" first appeared in the United States newspapers. The system was described by its large south-facing windows.	A Chicago newspaper	[33]
		1932	The first solar house known as "House of Tomorrow" was built. The system showed the ability to absorb and store heat energy (thermal mass).	Architects G & W Keck	[33]
4.	1930s	1933	The other solar house known as "Crystal House" at the Chicago World Fair was also built. The system showed the ability to absorb and store heat energy (thermal mass).	Architects G & W Keck	[33]
		1938	The inception of modern research into solar heating at the Massachusetts Institute of Technology (MIT). This program revealed that the collector performance calculations were developed.	Godfrey L. Cabot	[34]
		—	The invention of the system used solar collectors to heat air and then pumped it into a granulated rock-filled storage container.	K Miller	[33]
5.	1940s-1950s	1946-1949	The exploration of the new ground SAH system application used solid chemical compounds to absorb energy and subsequently release the heat by fusion when transformed from the solid state into the liquid state. This phase change material (PCM) technology has many applications in the industry.	Two residences in Massachusetts	[32, 33]
		—	The improved systems made several innovations to the previous solar collector design to further substantiate their true potentials.	The Americans	[33]
6.	1950s	1955	They developed and evaluated the efficiency of a 100% Arizona desert solar-heated house in the US. In the design, a flow-through air heater matrix and thermal energy storage (TES) system were used. Although the as-built system did not indicate an economic optimum, a smaller system using some other ancillary energy sources resulted in a lower optimum cost.	Bliss	[32, 35]
		1959	The construction of a dwelling near Denver used transparent glass plate collectors and a TES pebble bed design.	Lof	[32, 35]
		1963, 1964, 1976, 1978	The performance of the above system (a dwelling near Denver, 1959) was significantly studied.	Lof et al.	[32, 35]
7.	1960s-1970s	1968	Described how another type of SAH partially heated a laboratory building in Australia. The system was a 56.0 m^2 vee-grooved SAH that incorporated pebble bed storage.	Close et al.	[34]
		1970	Many different types of air heating systems have been experimentally constructed, and the performance of some has been evaluated and reported worldwide.	—	[32]
8.	2000s	2003	Studied the optimization designs of assorted European "solar combisystems."	Weiss et al.	[36]
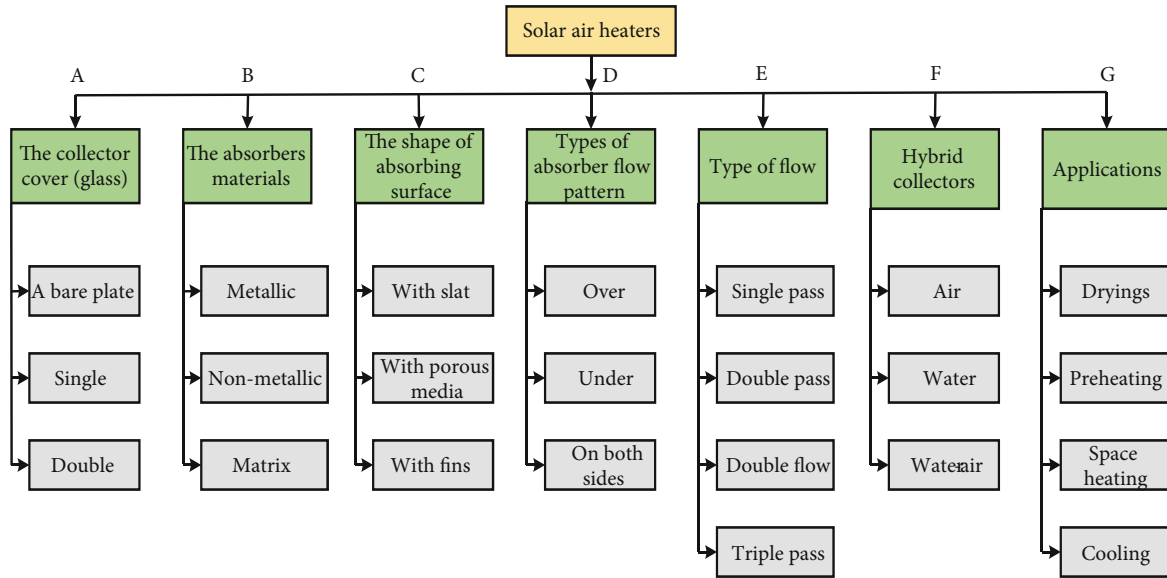
FIGURE 3: Distribution of solar air heaters based on Ghritlahre et al. [37].

beneficial application because it explicitly matches cooling demand with peak incident solar radiation.

In [61], the authors assessed the economic and environmental importance of solar cooling systems under Morocco's weather conditions. They generally concluded that the results of the solar cooling systems in hot climates could be used as an alternative to reduce the carbon footprint and provide an energy saving solution. Nevertheless, they further remarked from their research that the high installation cost is still the main obstacle facing the implementation of solar air conditioning systems. By 2020 and using the same Morocco case study, Dardouch et al. [62] proposed a simple, effective, and well-equipped solar air conditioning system. The system was equipped with a distillation column to purify the ammonia leaving the boiler that negatively affects the performance of the machine. In the study, they used the computer modeling and numerical simulation of the distillation absorption column machine and compared the results with the machine without a distillation column. Comparative results showed that the machine equipped with a distillation column is highly recommended due to its low energy usage level.

Generally, the energy consumption of buildings and industry has become a global issue [63]. Isaac and van Vuuren [64] show that energy demand for cooling is projected to rise rapidly in the whole of the twenty-first century due to climate change and increasing income in developing countries. Their study also reveals that global energy for cooling in buildings will overtake demand for heating in the long term. Also, the demand for heating will slightly increase too. According to Reyna and Chester [65], increasing renewable energy and energy efficiency quotas can significantly improve energy use by reducing the energy demand for cooling and heating. Therefore, SAHs can be a part of other renewable energy systems that promise to reduce carbon dioxide emissions in the 21st century.

3.4. Effectiveness of Solar Air Heaters. Thermohydraulic efficiency plays a decisive role in designing an energy-efficient SAH. According to a recent study by Rajarajeswari and Sreekumar [66], it was noted that while thermohydraulic effectiveness gives an impression about the pressure developed in the duct, the thermal efficiency suggests the heat transfer in the duct. The following analyses generally permit the estimation of the thermal and thermohydraulic efficiencies of SAH.

3.4.1. Thermal Performance

(1) Energy Analysis. The brief overview of the SAH energy performance analysis has been restated and reported by various authors since the 19th century, for instance, Tyagi et al. [67] in 2012, Oztop et al. [68] in 2013, and Ghritlahre et al. [37] at the end of 2019. Basically, energy analysis is a superior efficiency solar radiation that is transformed into heat at a specified frequency range and intensity. The incident energy on the evacuated tube is [37, 69]

$$\dot{Q}_c = I A_c, \qquad (1)$$

where $\dot{Q}_c$ is the energy incident on the evacuated cube (W), I is the solar radiation intensity on a surface area (W/m^2), and A_c is the absorber plate area (m^2).

Useful energy gained from collector $\dot{Q}_u$ is given by the following equation [69]:

$$\dot{Q}_u = \alpha \tau I A_c, \qquad (2)$$

where α is the inner surface absorptance of the evacuated collector tube coefficient and τ is the collector tube transmittance.
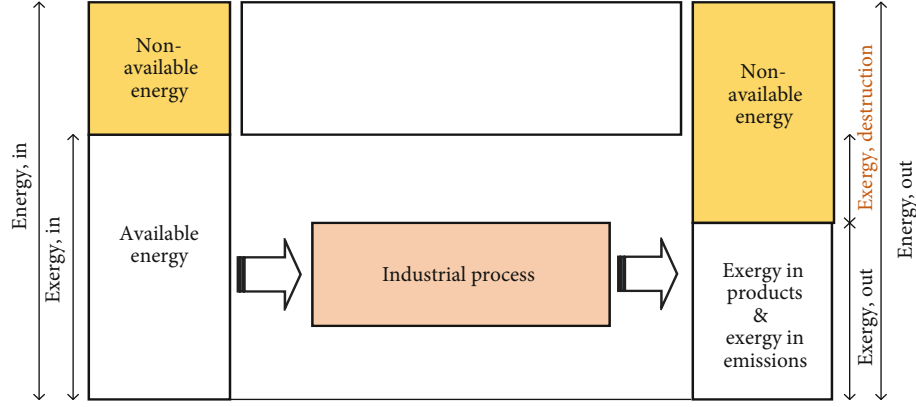
FIGURE 4: Basic concept of the overall balance of energy and exergy [72].

The absorbed useful energy transmitted through the fluid is assessed by energy conservation [37, 68–70]:

$$\dot{Q}_u = \dot{Q}_f = \dot{m}_f C_p \Delta T, \qquad (3)$$

where $\dot{Q}_f$ is the useful fluid energy, $\dot{m}_f$ is the fluid mass current, C_p is the fluid effective heat capacity, and ΔT is the fluid temperature change.

The thermal efficiency of solar air collectors is the ratio between useful heat and incident energy on the dryer or evacuated tube. Finally, the efficiency η of the collector system is determined as below [37, 68, 69]:

$$\eta = \frac{\dot{Q}_f}{\dot{Q}_c} = \frac{\dot{m}_f C_p \Delta T}{I A_c}. \qquad (4)$$

(2) Exergy Analysis. The concept of analyzing the exergy is the most useful for optimal energy use in any system. Additionally, this concept is mainly used to plan the design and operations of industrial processes. Thus, exergy effectiveness is the exergy proportion obtained through fluid flow to the exergy gained by the system [37, 71]. It could help in SAH design optimization to operate at a better efficiency. In recent years, Taheri et al. [72] conducted painstaking research on exergy analysis in process optimization for energy savings using the thermal spray approach. But interestingly, they also explained the concept of overall energy and exergy balance for a system using their novel hypothesis, as shown in Figure 4. Their research orientation is highly appreciated.

Generally, energy and exergy balance forms are [37, 71, 73–76]

$$\sum \dot{E}_i = \sum \dot{E}_0,$$

$$\sum \dot{Ex}_i - \sum \dot{Ex}_0 = \sum \dot{Ex}_{dest}, \qquad (5)$$

or

$$\dot{Ex}_{heat} - \dot{Ex}_{work} + \dot{Ex}_{mass,in} - \dot{Ex}_{mass,out} = \dot{Ex}_{dest}, \qquad (6)$$

where $\sum \dot{E}_i$ are the inlet energy rate sums, $\sum \dot{E}_0$ is the sum of the outlet energy rate, $\sum \dot{Ex}_i$ are the inlet exergy rate sums, $\sum \dot{Ex}_0$ is the outlet exergy rate sum, and $\dot{Ex}_{dest}$ is the rate of exergy destruction. In Equation (6), $\dot{Ex}$ and $\dot{E}$ are the energy and exergy, respectively, and "in" and "out" stand for the inlet and outlet of the system, respectively.

By Equation (6), the general exergy rate balance becomes

$$\sum \left(1 - \frac{T_a}{T_s}\right) \dot{Q}_c - \dot{W} + \sum \dot{m}_i \psi_i - \sum \dot{m}_0 \psi_0 = \sum \dot{Ex}_{dest}, \qquad (7)$$

where T_a and T_s are the ambient and sun temperatures, respectively, $\dot{W}$ is the work rate or work power, and ψ is the effective exergy, which becomes

$$\psi_i = (h_i - h_a) - T_a(s_i - s_a), \qquad (8)$$

$$\psi_0 = (h_0 - h_a) - T_a(s_0 - s_a), \qquad (9)$$

where h and s are the effective enthalpy and effective entropy, respectively.

Substituting Equations (8) and (9) into Equation (7) becomes

$$\left(1 - \frac{T_a}{T_s}\right) \dot{Q}_c - \dot{m}[(h_0 - h_i) - T_a(s_0 - s_i)] = \sum \dot{Ex}_{dest}, \qquad (10)$$

where T_a and T_s are the ambient and sun temperatures, respectively.

$$\dot{Q}_c = I A_c. \qquad (11)$$

The air enthalpy and entropy changes become

$$\Delta h_{air} = h_0 - h_i = C_{pf}(T_{fo} - T_{fi}), \qquad (12)$$

$$\Delta s_{\text{air}} = s_0 - s_i = C_{\text{pf}} \ln \frac{T_{\text{fo}}}{T_{\text{fi}}} - R \ln \frac{P_0}{P_i}, \tag{13}$$

where C_{pf} is the specific heat, T_{fo} is the output fluid temperature, T_{fi} is the initial fluid temperature, P_i is the initial fluid pressure, P_0 is the output fluid pressure, and R is the ideal gas constant.

Rearrangement of Equations (10)–(13) becomes

$$\begin{aligned}
&\left(1 - \frac{T_a}{T_s}\right) I A_c - \dot{m} C_{\text{pf}} (T_{\text{fo}} - T_{\text{fi}}) \\
&+ \dot{m} T_a \left(C_{\text{pf}} \ln \frac{T_{\text{fo}}}{T_{\text{fi}}} - R \ln \frac{P_0}{P_i} \right) = \sum \dot{\text{Ex}}_{\text{dest}}.
\end{aligned} \tag{14}$$

Finally, the exergetic efficiency or the second law of thermodynamics efficiency η_{II} of SAH can be obtained from the system's ratio of net exergy output to exergy input [37, 69, 73].

$$\eta_{\text{II}} = \frac{\dot{\text{Ex}}_0}{\dot{\text{Ex}}_i} = \frac{\dot{m}[(h_0 - h_i) - T_a(s_0 - s_i)]}{(1 - T_a/T_s) I A_c}. \tag{15}$$

3.4.2. Hydraulic Performance. As indicated in the earlier research studies, the thermal performance does not account for the pumping power loss; hence, thermohydraulic or efficiency criteria should be considered for the optimum design [77]. There is little known specifically published literature on the hydraulic performance of SAHs. Fortunately, a recently published paper on matrix solar air heaters [66] has a short discussion on the hydraulic performance of SAHs. According to their study, it was observed that the pressure drop developed in the air duct of SAHs is due to artificial roughness and other modifications in the flow duct as part of increasing heat transfer. Hydraulic performance is certainly necessary for increasing the efficient design of SAHs. Moreover, the earlier study by Kreith and Grove [78] reported that the pressure drop is related to the friction factor, as

$$f = \frac{(\Delta P) D_{\text{h}}}{2 \rho L v^2}, \tag{16}$$

where f is the friction, D_{h} is the hydraulic or correspondent width (m), ΔP is the pressure drop (Pa), ρ is the air density (kg/m³), L is the duct length (m), and v is the air velocity (m/s).

3.4.3. Thermohydraulic Performance. As mentioned above, thermohydraulic efficiency measurement is important for assessing SAH performance. To evaluate the overall system performance, the principle is to simultaneously examine both the hydrodynamics and the heat transfer [79]. The collector's thermohydraulic performance was popularized by Webb and Eckert [80]. Thus, the thermohydraulic performance of a coarse SAH is expressed as follows [79–85]:

$$\text{Thermohydraulic performance} = \frac{(\text{Nu}/\text{Nu}_s)}{(f/f_s)^{1/3}}, \tag{17}$$

where Nu and Nu_s indicate the roughened duct and smooth duct Nusselt numbers, respectively, while f_s and f are the smooth duct and roughened duct friction components, respectively.

According to our survey, there is plenty of specific published literature on SAH thermohydraulic efficiency since the year 2000. Nevertheless, Table 2 below summarizes the very recent important published literature on SAH thermohydraulic performance in the last 5 years and their brief descriptions. In Table 2 below, Equation (17) was taken as the general equation for the thermohydraulic performance of SAH. However, this equation can be slightly modified to support the new type of design of the solar heater.

3.4.4. Techniques Used to Enhance the Performance of Solar Air Heaters. The performance enhancement of SAH has been well studied by many researchers and institutions for many years. To achieve SAH performance improvement, several techniques have been used, like the effect of heat storage materials, absorber coating, packed beds, fins or corrugated surfaces, and artificial roughness. These techniques and recent relevant studies are briefly described in the following subsections.

(1) The Use of Heat Storage Materials. Developing techniques for energy storage is as important as the techniques for energy conversion. Energy storage is extremely important not only for energy conservation but also for enhancing energy conversion systems' reliability and efficiency [100, 101]. Thus, energy storage is extensively used in fields including variation in solar energy and significant differences between the day and night temperatures [100]. The integration of SAHs with an energy storage system may cause SAHs to be extensively applied. As shown in Figure 5 below, SAH energy storage substances are categorized as either hidden or heat exchange without phase change processes.

Phase change materials (PCMs) are the most well-known thermal storage materials. Isothermal PCMs present greater energy storage density and can serve under a variety of temperature ranges [102]. Batteries are used for energy storage. Scientists and practitioners are intensively using PCMs in different applications as a promising alternative to recover the heat of solar systems because of the energy storage limitations of batteries. According to a study by Mofijur et al. [102], PCMs are categorized into liquid-gas, solid-gas, solid-liquid, and solid-solid. But, solid-liquid PCMs are best suited for thermal energy storage. Moreover, solid-liquid PCMs are categorized into synthetic and organic PCMs and eutectics. In Table 3, the very recent previous publications on the use of heat storage materials were shown.

(2) The Use of Absorber Coating. The application of coatings of certain materials on the absorber surface is an effective way

TABLE 2: Recent important publications on solar air heaters using the thermohydraulic performance principle (2016-2020).

S. no.	Author(s) and year(s)	Computational domain	Description of the solar air heater system (model 2D/3D +turbulence model, algorithm)	Thermohydraulic performance	Other important remarks	References
1.	Kumar and Kim (2016)	Multi-V-type perforated baffles	3D model (of the flow domain), ANSYS FLUENT 6.3.26, CFD, RNG k-ε disturbance model, SIMPLE algorithm	The maximum baffle width was 5.0.	Reynolds number: 3000 to 10,000. The average Nusselt number rises while the average friction component reduces with the Reynolds number. The 3D CFD analysis showed a positive outcome, and the CFD model is highly recommended for the rectangular channel baffle shape analysis. The investigated system showed good numerical optimal results with the experimental data.	[86]
2.	Gawande et al. (2016)	Reverse L-shaped ribs	2D CFD analysis SAH duct, ANSYS FLUENT 14.1, CFD code, RNG k-ε disturbance model, SIMPLE algorithm	It varied between 1.62 and 1.9.	Reynolds number: 3800 to 18,000. The increasing Reynolds number increases with the average Nusselt number. The average friction component decreases with the increasing Reynolds number. The CFD theory and analytical results compared favorably with experimental results.	[87]
3.	Gill et al. (2017)	Broken arc ribs in a rectangular duct	3D periodic geometries of the roughened duct, ANSYS Academic Research CFD 15, RNG k-ε turbulence model	1.94 at maximum	Reynolds number: 2000 to 16,000. The Nusselt number, friction coefficient, and thermohydraulic efficiency were enhanced.	[88]
4.	Singh (2017)	Arched absorber plate using turbulators	2D CFD model with the plane, ANSYS FLUENT (v16.2), RNG k-ε turbulence model, SIMPLE algorithm	The value was clearly illustrated in the figure.	Reynolds number: 3800 to 14,000. The Nusselt number significantly improved at a high Reynolds number above 10,000. The study concluded that the arched shape design of the SAH absorber plate remarkably enhanced overall efficiency.	[89]
5.	Thakur et al. (2017)	Novel hyperbolic rib geometry	2D CFD simulation, ANSYS FLUENT 15.0 CFD code, RNG k-ε model, SIMPLE algorithm	The value was clearly illustrated in the figure.	At a very high Reynolds number, the heat transfer rate was more noticeable in rectangular ribs than the pressure drop effect, which causes an overall increase in thermohydraulic performance.	[90]
6.	Gawande et al. (2018)	Various rib shapes (slanting, right-angled triangular, and reverse L-shaped ribs)	2D roughened computational domain SAH, ANSYS FLUENT 14.5 CFD code, RNG k-ε model, SIMPLE algorithm	20° chamfered: from 1.577 to 2.047 Right-angled triangular rib: from 1.41 to 2.03 Reverse L-shaped rib: from 1.62 to 1.90	Reynolds number: 3800 to 18,000. The obtained values in the thermohydraulic performance column were achieved under the following conditions: 15,000 Reynolds number and 0.042 relative roughness height. In brief, it was clear that the specific thermal efficiency incremented in ascending order from the 20° slanted rib to the right-angled triangular rib and reverse L-shaped rib.	[91]

Table 2: Continued.

S. no.	Author(s) and year(s)	Computational domain	Description of the solar air heater system (model 2D/3D +turbulence model, algorithm)	Thermohydraulic performance	Other important remarks	References
7.	Kumar and Layek (2018)	Absorber plate twisted rib	A duct with dimensions of 2640 mm × 160 mm × 40 mm was constructed from plywood.	2.13	Reynolds number: 3500 to 21,000. The optimum thermohydraulic performance of 2.13 was obtained at 21,000 Reynolds number.	[92]
8.	Manjunath et al. (2018)	Sinusoidal corrugations on the absorber plate	3D CFD simulation, SST k-ω turbulence model, SIMPLE segregated solver	The metric was clearly illustrated in the figure.	Reynolds number: 4000 to 24,000. The thermohydraulic performance of all configurations exhibits higher values when compared to the previous base model. This was obtained by lower flow rate conditions. This study finally revealed that the SAH thermohydraulic performance is significantly influenced by the aspect ratio and wavelength of the sine wave corrugated absorber plate.	[93]
9.	Patel and Lanjewar (2018)	Staggered rib roughness combined with multiple discrete V-designs	The rectangular duct of 200 mm × 25 mm flow cross-section.	1.55 at maximum	Reynolds number: 3000 to 12,000. The staggered rib combined with multiple discrete V-designs had greatly improved thermal efficiency.	[94]
10.	Menni et al. (2019)	Plane rectangular combined V-shaped floor channel SAH having various ribs	CFD software FLUENT, k-ε disturbance model, Finite Volume Method (FVM), Standard k-epsilon turbulence model (k-ε), SIMPLE algorithm	The metric was clearly illustrated in the figure.	Reynolds number: 12,000 to 32,000. Among the various ribs (equilateral-triangular, trapezoidal, triangular pointing downstream, triangular pointing upstream, and square), the triangular pointing downstream was the optimal operating system. The ribs of the lower surface of the upper hot wall greatly increase the internal heat transfer efficiency of the channel.	[95]
11.	Bezbaruah et al. (2019)	Modified forms of conical vortex generators	3D model, ANSYS FLUENT 18.0, a commercial CFD tool, 5 turbulence models (ideal k-ε, recognizable k-ε, RNG k-ε, SST k-ω, and ideal k-ω design), SIMPLE algorithm	1.06 at maximum	Reynolds number: 3000 to 15,000. This study revealed that the maximum 1.06 thermohydraulic performance was for half-canonical vortex generators at 60° attack angle and 1.02 for canonical vortex generators.	[96]
12.	Sivakandhan et al. (2020)	Inclined rib roughness	A mathematical model was developed by authors.	The value was clearly illustrated in the figure.	The study analytically improved the thermohydraulic performance of a new hybrid duct SAH. The results showed that the analyzed system highly improved the thermal and effective (thermohydraulic) efficiencies past 22.4% and 18.1%, respectively, when correlated with the traditional parallel pass rectangular duct solar air heater.	[97]

TABLE 2: Continued.

| S. no.	Author(s) and year(s)	Computational domain	Description of the solar air heater system (model 2D/3D +turbulence model, algorithm)	Thermohydraulic performance	Other important remarks	References
13.	Bensaci et al. (2020)	Different baffle positions	3D geometry, a numerical model based on CFD, ANSYS FLUENT 15.0, classical turbulence k-ε models (ideal k-ε, RNG k-ε, recognizable k-ε, and k-ω designs), SIMPLE numerical algorithm	0.75 at maximum	Reynolds number: 2370 to 8340. This study discussed and analyzed the performance of four cases of different baffle positions. Then, the second case where baffles are located in the first half of the air channel (50 percent down) was recommended as the optimum configuration. After their CFD analysis, the RNG k-ε disturbance prototype was also selected for its qualitative agreement and good accord with Dittus-Boelter and modified Blasius correlations.	[79]
14.	Dezan et al. (2020)	Irregular rows of rectangular winglet pairs	The flow was three-dimensional, ANSYS FLUENT 19.1 commercial code, k-ω SST turbulence model	The value was clearly illustrated in the figure.	Reynolds number: 5000 to 10,000. The thermohydraulic efficiency of a SAH duct among rectangular winglet pairs was investigated. Thus, in all cases investigated, the study revealed that the thermohydraulic efficiency that was not systematically mounted on the channel exceeded those of fixed interval plans.	[98]
15.	Nidhul et al. (2020)	V-ribs	3D CFD simulation, ANSYS v19.0, RNG k-ε turbulence model, SIMPLE algorithm	2.01 at maximum	Reynolds number: 5000 to 20,000. This study used the CFD and exergy analysis of triangular duct V-rib SAH applying the given Reynolds number. The new SAH architecture improves the overall performance when compared to other artificial roughness employed in the triangular duct solar air heaters.	[99]
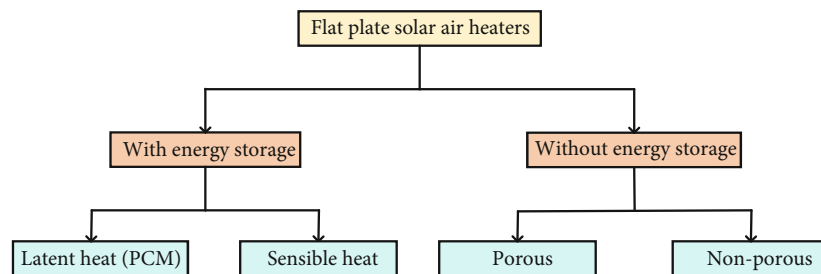
FIGURE 5: Classification of flat plate SAHs: without and with energy storage.

to increasingly harness solar insolation. As shown in Figure 6, coatings are generally categorized as selective and nonselective coatings.

Nonselective coatings have poor solar selectivity and are also thermally unstable at high temperatures, which results in poor absorber efficiency. Some of the examples of nonselective coatings are black paints and urethane paints. A coating should have a high absorptivity but low emissivity in the solar thermal application so that it can maintain the trapped thermal energy [103]. That is why the application of nonselective coatings for solar thermal conversation technology

TABLE 3: Summary of very recent research studies on techniques used to improve the efficiency of SAHs.

Techniques used to improve the performance of SAHs and their types		Studies	Years
Methods	Types/description of the method		
Heat storage materials	Sensible heat storage materials (water, pebble, bed, sand, gravel, metal chips, and concrete)	Murali et al. [117], Kalaiarasi et al. [17], Vijayan et al. [118], Ayyappan et al. [119], and Kalaiarasi [76]	2015-2020
	Latent heat storage materials (PCM): paraffin wax, Glauber's salt, eutectics of organic and nonorganic compounds, and fatty acids	Javadi et al. [120], Karthikeyan et al. [121], SunilRaj and Eswaramoorthy [122], Raj et al. [123], Sharma et al. [124], Mahmoud et al. [125], and Jawad et al. [126]	2020
Absorber coating	Nonselective coating and selective coating	Abdelkader et al. [127] and Kumar et al. [128]	2019-2020
Packed bed	Single-pass packed bed	Dhiman and Singh [129] and Singh [130]	2015-2020
	Double-pass packed bed	Singh et al. [131], Singh [130], Dosapati and Mandapati [132], Roy and Hoque [133], Chouksey and Sharma [134], Priyam et al. [135], Singh and Dhiman [136], and Mahmood et al. [137]	2015-2020
Fins or corrugated surfaces	Longitudinal fins, attaching baffles, and corrugated fins	Kumar and Chand [138], Handoyo et al. [139], Aboghrara et al. [140], Kabeel et al. [141], Darici and Kilic [142], Priyam and Chand [105], Lin et al. [143], and Zheng et al. [144]	2015-2020
Roughness geometry	Coarse transverse rib	Singh et al. [145], Singh and Singh [146]	2015-2020
	Coarse V-rib	Nidhul et al. [99], Jain and Lanjewar [147], Singh and Lanjewar [148]	2015-2020
	Coarse transverse wedge-shaped rib	Bhagoria et al. [149]	2002
	Coarse rib-grooved	Jaurker et al. [150]	2006
	Coarse metal grit rib	Karmare and Tikekar [151]–[153]	2007-2010
	Coarse arc-shaped rib	Ghritlahre et al. [154], Kumar et al. [155], Ghritlahre and Prasad [156], Sahu and Prasad [157], Saravanakumar et al. [158, 159], and Yadav and Prasad [160]	2015-2020
	Coarse discrete W-shaped rib	Jain et al. [161]	2017
	Coarse multi-V-rib	Jin et al. [162], Kumar and Kim [163]	2015-2020
	Coarse W-shaped rib	Patel and Lanjewar [164], Thakur and Thakur [165]	2015-2020
	Coarse discrete V-down rib	Singh et al. [166]	2012
	Staggered ribs connected coarse broken V-rib	Patil et al. [167, 168]	2010-2015
	Coarse dimple-shaped rib	Sethi et al. [169]	2012
	Coarse circular protrusions organized circular arc rib	Yadav et al. [170]	2013
	Coarse gap multi-V-shaped rib	Kumar et al. [171]	2013
	Coarse multi-arc-shaped rib	Singh et al. [172]	2014
	Coarse V-rib connected symmetrical gaps	Maithani and Saini [173]–[175]	2015-2020
	Coarse staggered rib linked multigap V-down ribs	Deo et al. [176]	2016
	Coarse reverse L-shaped rib	Gawande et al. [87]	2016
	Coarse gaps linked multiple arc-shaped rib	Pandey et al. [177]	2016
	Coarse broken arc rib	Gill et al. [88] and Hans et al. [178]	2015-2020
	Staggered rib piece connected broken arc rib	Gill et al. [179]	2016
	"S"-shaped pattern organized arc-shaped ribs	Kumar et al. [180]	2017
	Dimpled barrier multiple type V-pattern rib	Kumar et al. [181]	2017

TABLE 3: Continued.

| Techniques used to improve the performance of SAHs and their types | | Studies | Years |
Methods	Types/description of the method		
	Hyperbolic ribs	Thakur et al. [90, 182]	2015-2020
	Inclined upper part connected rectangular stopper rib	Menasria et al. [183]	2017
	Wobbled multiple V-shaped ribs	Jin et al. [184]	2017
	Thin truncated ribs	Sharma and Kalamkar [185]	2017
	SAH with helical flow paths	Heydari and Mesgarpour [111], Bezbaruah et al. [113], and MesgarPour et al. [110]	2018-2020
Helical or spiral flow path	SAH with the spiral shape of spoilers	Jia et al. [112]	2018
	SAH equipped with helical coiled inserts	Singh and Vardhan [114]	2019
	SAH integrated with helical tubes carrying PCM	Saxena et al. [115]	2020
	SAH tube with helical corrugation and perforated circular disc inserts	Bhattacharyya et al. [116]	2020
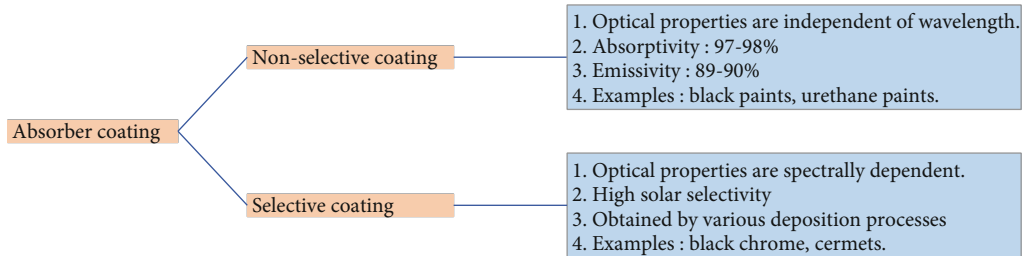
FIGURE 6: Classification of solar coatings and their properties [103].

still has some limitations. By considering the last six years since 2015, there are a few publications of nonselective coatings in the solar field. However, those coatings are given less attention by researchers. On the other hand, solar selective coatings in different spectral regions have differing absorptivity and emissivity. A recent detailed review on the performance improvements of solar collectors by Suman et al. evidently shows that these coatings are spectrally dependent [103]. Their study also highlights how solar selective coatings allow for the passage of incoming solar radiation and block the emittance of longer thermal wavelength radiation. Therefore, solar collectors help to capture the radiative energy to reach high temperatures. Black chromes and cermets are some of the examples of selective coatings. In Table 3, the very recent previous publications on the use of absorber coating were shown.

(3) The Use of Packed Beds. In using a packed bed, airflow into the bed from the collector charges the batteries. The discharge process occurs by reversing the airflow. Packed beds have a long lamination time because poor heat transfer by conduction occurs between bed layers. Therefore, charge and discharge are mutually exclusive when a rock bed is used. However, the laminated rock bed system is as efficient as comparable water storage systems for nighttime distribution to the load [100]. Also, Kumar and Kim [104] extensively reviewed SAH and energy storage systems comprising single- and double-pass packed beds. The study indicates that the

thermal efficiency of the double-pass packed bed SAH was greater than that of the single-pass packed bed SAH. In Table 3, the very recent previous publications on the use of packed beds were shown.

(4) The Use of Fins or Corrugated Surfaces. Extended surfaces like fins or corrugated surfaces increase the heat transfer percentage without increasing the capacity [105, 106]. Kabeel et al. [107] empirically examined the efficiency of a glassy bladed single-pass entrance SAH including nineteen longitudinal fins. Moreover, results for evaluating the proposed SAH performance that contrasted against the traditional SAH indicate the daily maximum efficiency of 57.0% at 0.04 kg/s and 8.0 cm fin height for the modified finned SAH. Also, the daily maximum efficiency for the conventional SAH was around 32.0%. In Table 3, the very recent previous publications on the use of fins or corrugated surfaces were shown.

(5) The Use of Artificial Roughness. The heat transfer proportion within the absorber surface and airflow determines the efficiency of the flat surface SAH. But higher thermal resistance increases the absorber surface temperature for higher heat loss to the environment. The little heat transfer proportion arises because of the artificially roughened laminar thickness caused by the heat transfer surface [108]. The laminar sublayer was disturbed in the conventional flat plate SAH to enhance heat exchange of the absorber surface. This
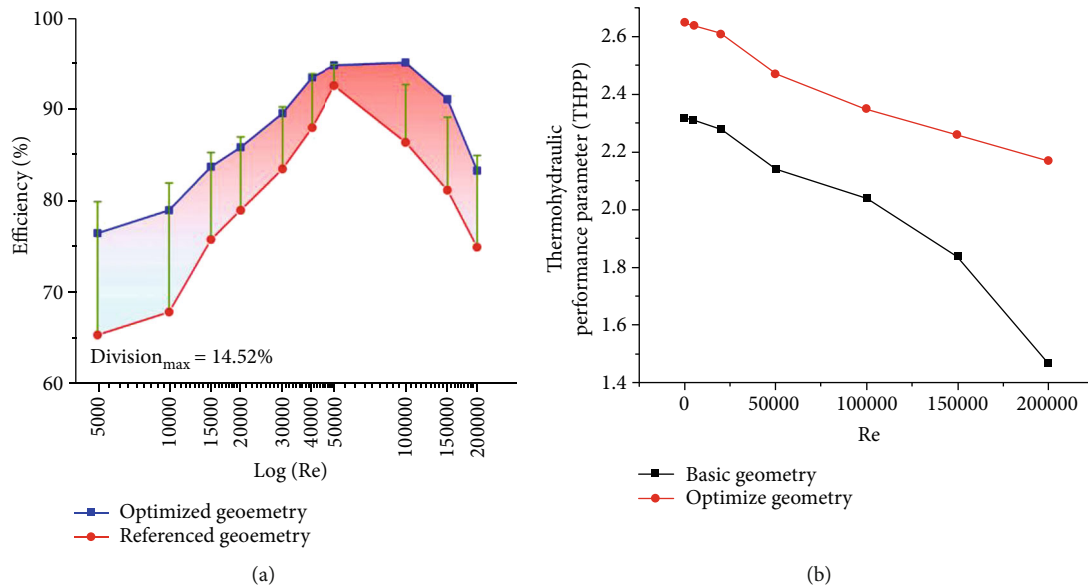
FIGURE 7: Illustration of energy efficiency and thermohydraulic performance parameters for reference and optimized geometries: (a) energy efficiency comparison for different Reynolds numbers and (b) thermohydraulic performance parameters for SAHs for different Reynolds numbers [110].

is adequately implemented using artificial ribs at the absorber's airflow side [83].

Artificial roughness is widely researched for the enhancement of SAH performance. In recent years, some extensive review papers have been written to provide a comprehensive understanding of SAH improvement using artificial roughness. In 2015, Lanjewar et al. [108] reviewed the progress of the artificially roughened heat exchange improvement in SAH by examining the efficiency of distinct orientations for roughened double arc ribs. In the same year, Sharma and Kalamkar [81] surveyed the thermohydraulic efficiencies of SAHs possessing artificial roughness. This comparative study was conducted to evaluate the various roughness elements of absorber surfaces in SAHs. In 2018, Singh and Singh [83] presented a detailed analysis of artificially roughened configurations used in SAHs. In the same year, Singh et al. [109] conducted an empirical study of artificially roughened SAHs. This article presented heat exchange and friction parameters of distinctly roughened geometries in artificially roughened SAHs. By 2020, a new study by Araújo [82] considered recent publications of the last ten years, using semiempirical investigations. The study generally concluded that the multiple V-shaped ribbed gap absorbers provided the most optimal roughened configuration. In Table 3, the very recent previous investigations on the use of artificial roughness were illustrated.

(6) The Use of Helical or Spiral Flow Paths. Above all, in Ref. [110], the authors indicate that the improvement of the air adsorbent contact area of the SAH, including higher retention time, enhances the heat transfer performance. In this very study, the double-pass SAH optimization among helical flow paths was investigated. The results of their study then showed that for all Reynolds numbers, the optimized geom-

etry led to a significantly greater thermohydraulic performance parameter compared to the simple one, as shown in Figure 7 below.

In 2018, Heydari and Mesgarpour [111] hypothetically and empirically presented the efficiency of helical channel flow paths in SAH. The double-pass SAH among helical channels was found to have 14.7% thermal efficiency above the SAH without helical channels and 8.6% above the pass-finned SAH. In a later study [112], the authors introduced a new type of SAH using the spiral shape of spoilers. After the experimental work, they concluded that the SAH spiral shape of spoilers has greater heat collection efficiency than the traditional and convoluted SAH.

In 2019, Bezbaruah et al. [113] numerically considered the finned absorber surface and helical flow path SAH thermal efficiency using a CFD analysis. The study outcome indicated that the maximum thermal performance enhancement of the new absorber plate design was 3.72 times more compared to its flat plate counterpart at the same mass flow rate. One year later, three studies were carefully conducted using various helical or spiral paths to enhance SAH efficiency. One investigation in [114] experimentally determined the efficiency of the Evacuated Tube Collector SAH comprising Helical Coiled Inserts (ETC-HI) SAH and the simple ETC SAH. Their experiments indicate that the ETC-HI SAH thermal efficiency was better and yielded higher air temperature than the simple ETC SAH. Furthermore, Saxena et al. [115] evaluated the thermal efficiency of a SAH integrated with PCM carrying helical tubes. In their work, three models of SAH were designed as briefly explained as follows: model SAH-A was the reference model of comparison; model SAH-B has helical tubes filled with low sensible heat storage material; and model SAH-C was the newly improved SAH-B model integrated with helical tubes filled with a specific

mixture of granular carbon powder and paraffin wax. The experimental results of the three models showed that, in comparison to SAH-A and SAH-B, SAH-C was the best model in terms of thermal efficiency. Lastly, a SAH tube with helical corrugation and perforated circular disc inserts was experimented and the heat transfer and exergy were both analyzed [116]. Their outcome indicated that in the presence of a perforated circular disc inside the helically corrugated tube, heat transfer was increased by around 50 to 60%. In brief, the authors recommended that their outcome can be conveniently used to implement a new design of the solar air heater and heat exchanger. Table 3 shows the very recent previous investigations on various rib geometries employed in SAHs.

In summary, there are currently a few published papers outlining the helical or spiral flow paths to enhance the performance of SAH or to increase the air retention time in SAH. However, to the best of our knowledge, the use of helical or spiral flow paths in SAH has shown good results, as discussed in the previous paragraphs of this subsection. Thus, it should be noted that the future research trend on the use of the helical or spiral flow paths in SAHs will likely be very competitive and beneficial. In Table 3, the very recent previous investigations on the use of helical or spiral flow paths were illustrated.

4. Metaheuristic Optimization Algorithms for Solar Air Heaters

Over the past few decades, recent advancements in computer science and mathematical optimization made metaheuristic algorithms useful for many applications. Unlike heuristics, they do not really need any problem-dependent heuristic information. One of the key advantages of metaheuristic algorithms is that they make few assumptions about the problem and try to regard it as a black box. Importantly, to search for the optimum solution, they sample the problem's search space which is too large to be fully searched [186].

Starting with the genetic algorithm (GA), studies [187–189] applied the GA in solar energy systems to obtain good potential solutions to optimization problems. The development of metaheuristic algorithms started with the GA, differential evolution (DE), and particle swarm optimization (PSO) algorithms [25]. The authors in [26, 190] again stated that metaheuristic algorithms have benefited from the search efficiency and/or accuracy, reduction of the computational burden, and high-quality solution of complex optimization problems. This section discusses some metaheuristic algorithms applied in SAH optimization.

4.1. Using Particle Swarm Optimization (PSO)

4.1.1. Basic Particle Swarm Optimization Algorithm. The PSO algorithm mimics the flocking nature of birds or fish schooling [186, 191–193]. Furthermore, the particle swarm follows the global and individual optimal directions for updating its velocity and position [25, 26]. The PSO method consists of three phases: initialization, exploration, and evaluation.

(1) Initialization. Define the size of the population and starts from a random particle.

(2) Exploration. The particle's current position "X_i" updates as they move with a velocity along the search space V_i. During the assessment process, the particle's current best position "P_{bi}" and the global optimal position "G_b" are documented. Every particle's location is upgraded utilizing Equation (18) below [25]:

$$X_i^{k+1} = X_i^k + V_i^{k+1}, \qquad (18)$$

where X_i^{k+1} is the updated location of the ith speck, X_i^k is the current location of the ith speck, and V_i^{k+1} shows the updated velocity.

The velocity of the ith particle is updated using the velocity update equation in Equation (19) below [25]:

$$V_i^{k+1} = W \cdot V_i^k + \left[r_1 C_1 \left(P_{bi} - X_i^k \right) \right] + \left[r_2 C_2 \left(G_b - X_i^k \right) \right], \qquad (19)$$

where the updated position of the particle is represented by X_i^{k+1}, X_i^k shows the current position of the ith particle, V_i^{k+1} shows the updated velocity, V_i^k is the current velocity, W is the inertial weight, C_1 is the individual proportion, C_2 is the communal quota, and r_1 and r_2 are arbitrary numbers in $[0, 1]$.

(3) Evaluation. In this phase, the particle's fitness value is evaluated to update the recorded data for "P_{bi}" and "G_b" as follows [25]:

$$\begin{aligned} P_{bi} &= X_i^k, \quad \text{if } f\left(x_i^k\right) \geq f(P_{bi}), \\ G_b &= P_{bi}, \quad \text{if } f(P_{bi}) \geq f(G_b). \end{aligned} \qquad (20)$$

More importantly, to understand the PSO algorithm better, its flowchart is in Figure 8.

4.1.2. Particle Swarm Optimization for Solar Air Heaters. Siddhartha et al. [14] used several PSO algorithm characteristics to optimize the thermal efficiency of a glossy flat plate SAH by considering glass cover plates, solar irradiance, tilt angle, plate emissivity, and Reynolds number. In their study, MATLAB software was used to carry out the simulation. Their results showed that the optimal thermal performance (72.42%) was obtained using 1.0 m/s wind velocity (V), 68.36° tilt angle, 0.89 plate emissivity, 280.43 K ambient air temperature, 3.0 glass cover number (N), and 600.0 W/m² solar irradiance (S). Empirical evidence also indicates that the algorithm is very robust.

In 2019, Kumar and Layek [84] extensively analyzed the thermohydraulic efficiency of roughened SAHs. The results of the experiment were analyzed with the help of MINITAB version 17 software. Moreover, two metaheuristic algorithms
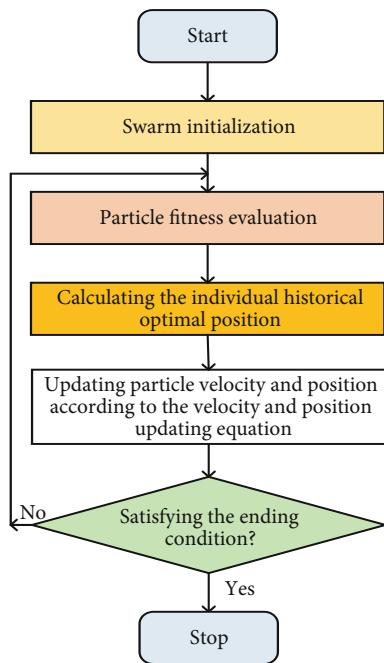
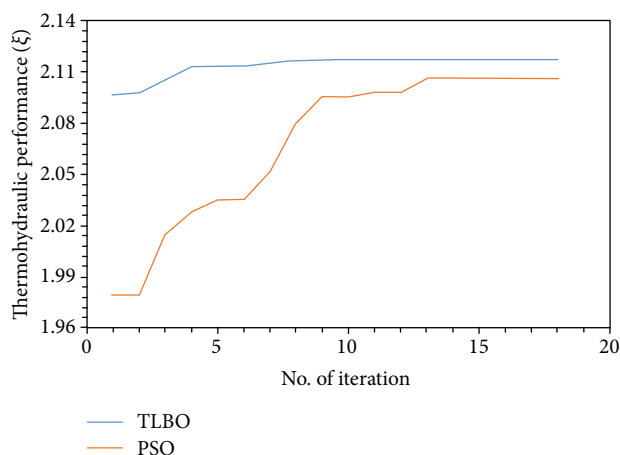FIGURE 8: Flowchart for the PSO algorithm.

FIGURE 9: Convergence plot of thermohydraulic performance for PSO and TLBO techniques [84].

(PSO and TLBO) were also considered to optimize the efficiency of the SAH. The maximum 2.13 empirical thermohydraulic efficiency considered the 3 twist ratio (y/e), 8 pitch-height ratio (P/e), 21,000.0 Re, and 60° rib inclination angle (α). As mentioned above, two metaheuristic evolutionary algorithms were appropriately applied to evaluate an optimal set of roughness combinations with operating parameters. As shown in Figure 9 and Table 4 below, the TLBO approach reveals better results for maximizing performance than the PSO technique. They concluded that, in terms of reliability, competence, execution, and global convergence, the simulated optimized results obtained from the TLBO algorithm were more satisfying with experimental data.

Motivated by the PSO's flexibility and adaptability to any difficult problem of optimization, researchers have

proposed many different variations of PSO to deal with SAH optimization. In this situation, the authors in [194] proposed a parametric three-sided roughened SAH multi-objective particle swarm optimization (MOPSO) algorithm. Their affirmatively validated optimal results indicate a 3.39% error. The parameters of this study are found in Table 4 below.

4.2. Using Teaching-Learning Based Optimization (TLBO)

4.2.1. Basic Concept of Teaching-Learning Based Optimization. The recent TLBO algorithm inspired by the teaching-learning procedure suggested by Rao et al. [195–197] and Rao [198] depends on teachers' influence on learners' productivity in class. Two learning approaches are described in this algorithm: (1) by teachers (teacher phase) and (2) through interaction with more learners (learner phase). The teacher makes the optimal result in the whole population. Actually, the design parameters are contained in the objective functions of the optimization problem, and the optimal solution is the objective function's finest result [197–199]. The TLBO algorithm flowchart is in Figure 10.

4.2.2. Teaching-Learning-Dependent Solar Air Heater Optimization. An extensive comparison between the PSO and TLBO techniques of roughened SAHs was made by Kumar and Layek [84] in 2019. This study has been discussed in the previous subsection, and it clearly revealed that the TLBO technique showed a higher optimal solution compared with the PSO approach. Rao and Waghmare [24] evaluated the thermal efficiency of the polished flat plate SAH by the TLBO approach. In the study, the TLBO code was developed in MATLAB and the thermal efficiency maximization of the glossy flat plate SAH was the objective function. The 76.67% highest thermal efficiency was achieved by the following inputs to the objective function: 1.2729 m/s wind speed, 59.5832° tilt angle, 0.8835 plate emissivity, 293.9362 K ambient temperature, 600.0 W/m^2 irradiance, 20,000.0 Reynolds number, and 2.1395 K temperature rise. The study authors concluded that the results from the TLBO algorithm were slightly higher, correspondingly similar to several optimization algorithms like GA, PSO, and simulated annealing (SA), as shown in Figure 11. Moreover, they also stated that the thermal efficiency increased with both the Reynolds number and the glass cover plate number.

Rao [200] again investigated the efficiency of the polished flat plate SAH applying the elitist teaching-learning-based optimization (ETLBO) and TLBO algorithms. ETLBO is a recent novel algorithm which was introduced by Rao and Patel [201] for constraint optimization, and it showed some improved results compared with TLBO. In the study above by Rao [200], the results perfectly showed that applying ETLBO, the 76.7881% highest optimal thermal efficiency was achieved with the following: 1.3194 m/s wind velocity, 60.4883° tilt angle, 0.8947 plate emissivity, 292.5993 K ambient temperature, 2.1448 K temperature rise, 600.0 W/m^2 irradiance, and 20,000.0 Reynolds number. The efficacy of the ETLBO and TLBO algorithms was assessed against

TABLE 4: Comparison of thermal or thermohydraulic performance of SAHs using various metaheuristic algorithms for SAH optimization.

S. no.	Author(s), year(s), and references	Types of SAHs	Metaheuristic algorithm(s)	Important considered input/design/operating parameters for optimal performance (efficiency)	Thermohydraulic/thermal performance (efficiency)	Comments
1.	Siddhartha et al. (2012) [14]	A smooth flat plate SAH (SFPSAH)	PSO	(i) Number of glass covers (N): 3 (ii) Solar irradiance (S): 600.0 W/m^2 (iii) Wind velocity (V): 1.0 m/s (iv) Tilt angle (β): 68.36° (v) Plate emissivity (dimensionless) (ε_p): 0.89 (vi) Ambient temperature of air (T_a): 280.43 K	The maximum thermal efficiency: 72.42%	(i) The increasing Reynolds number (Re) leads to a better heat transfer rate and enhanced thermal efficiency at $S = 600.0$ W/m^2. (ii) The thermal efficiency of SFPSAH was improved using a greater number of N and the same value of $S = 600.0$ W/m^2. (iii) The maximum thermal efficiency for three glass cover plates was found at Re = 20,000.0. (iv) By increasing the solar radiation intensity, the thermal performance decreased.
2.	Mohanty et al. (2020) [194]	A three-sided roughened SAH	MOPSO	(i) Re: 12,000.0–13,000.0 (ii) Applicable pitch roughness: 10.0 (iii) Applicable roughness height: 0.3–0.4 (iv) Mass flow rate : 0.04 kg/s	The greatest thermal efficiency range: 63.0–75.0%	(i) The Reynolds number and applicable pitch roughness were the most dominant parameters for both responses. (ii) The applicable roughness height had little variation effects on both responses. (iii) Both the enhanced Nusselt and Reynolds numbers weakened the applicable pitch roughness.
3.	Kumar and Layek (2019) [84]	A roughened SAH (twisted rib roughness)	PSO and TLBO	(i) Twist ratio (y/e): 3 (ii) Pitch-height ratio (P/e) : 8 (iii) Re: 21,000.0 (iv) Rib inclination angle (α): 60.0°	Experimentally, 2.13 was the highest thermohydraulic efficiency. The optimal results for the highest thermohydraulic efficiency obtained by PSO and TLBO techniques were 2.105 and 2.117, respectively.	(i) The optimum thermohydraulic efficiency was obtained at a lower (y/e) value and decreases with an increasing (y/e) ratio. (ii) The TLBO showed a better optimal solution than the PSO algorithm.
4.	Rao and Waghmare (2015) [24]	A smooth flat plate SAH	TLBO	(i) Wind velocity: 1.2729 m/s (ii) Tilt angle: 59.5832° (iii) Plate emissivity: 0.8835 (iv) Ambient temperature: 293.9362 K (v) Temperature rise: 2.1395 K (vi) Irradiance: 600.0 W/m^2	The maximum thermal efficiency: 76.67%	(i) The thermal efficiency increases with the Reynolds number. (ii) The thermal efficiency slightly increases with the glass cover plates. (iii) The solutions obtained from the TLBO algorithm were better than alternative metaheuristic algorithms like GA, PSO, and SA. Therefore, for the same considered problem, the

Table 4: Continued.

S. no.	Author(s), year(s), and references	Types of SAHs	Metaheuristic algorithm(s)	Important considered input/design/operating parameters for optimal performance (efficiency)	Thermohydraulic/thermal performance (efficiency)	Comments
5.	Rao (2016) [200]	A smooth flat plate SAH	TLBO and ETLBO	(vii) Reynolds number: 20,000.0 (i) Wind velocity: 1.3194 m/s (ii) Tilt angle: 60.4883° (iii) Plate emissivity: 0.8947 (iv) Ambient temperature: 292.5993 K (v) Temperature rise: 2.1448 K (vi) Irradiance: 600.0 W/m^2 (vii) Reynolds number: 20,000.0	The highest thermal efficiency: 76.7881% (applying ETLBO)	TLBO was better than alternative optimization techniques in the newly published literature. (i) The thermal efficiency increases with the Reynolds number. (ii) The thermal efficiency slightly increases with glass cover plates. (iii) The ultimate solutions obtained from the TLBO and ELTBO algorithms were better than alternative metaheuristic algorithms like GA, PSO, and SA. Hence, TLBO and ELTBO algorithms were found to be more effective.
6.	Varun and Siddhartha (2010) [202]	A smooth flat plate SAH	GA	(i) Air velocity: 2.95 m/s (ii) Tilt angle: 65.33° (iii) Plate emissivity: 0.86 (iv) Ambient temperature: 296.11 K (v) Temperature rise: 2.20 K (vi) Irradiance: 600.0 W/m^2 (vii) Reynolds number: 20,000.0	The highest thermal efficiency: 75.65%	(i) The thermal efficiency of a flat plate SAH increases with the Reynolds number. (ii) The highest thermal efficiency was obtained applying many system design parameters.
7.	Şahin (2012) [203]	SAC	ABC and GA	(i) Velocity: 3.6859 m/s (ii) Collector slope: 40° (iii) Absorber plate emissivity: 0.9415 (iv) Emissivity of glass covers: 0.8043 (v) Air temperature: 290.0798 K (vi) Irradiance: 600.0 W/m^2 (vii) Reynolds number: 6,000.0	The optimum thermal efficiency: (i) ABC: 0.7998 (ii) GA: 0.7983	(i) ABC and GA optimization solutions were more precise than traditional methods. (ii) The results show that both the ABC and GA techniques were profitably applied for the thermal SAC efficiency optimization. However, the ABC algorithm was preferable to the GA. (iii) The thermal efficiency of a SAC increases with the Reynolds number.
8.	Saravanakumar et al. (2020) [159]	Joined fins and stopper coarse arc-shaped rib SAH	GA	(i) Fin number: 8 (ii) Baffle length: 0.2 m (iii) Baffle width: 0.015 m (iv) Mass flow rate: 0.012 kg/s	The highest exergy efficiency: 5.2%	(i) Higher optimum thermal efficiency leads to a greater mass flow rate, and more exergy destruction is observed between the plate and the sun. (ii) Exergy efficiency was assessed based on exergy destruction and losses.

TABLE 4: Continued.

S. no.	Author(s), year(s), and references	Types of SAHs	Metaheuristic algorithm(s)	Important considered input/design/operating parameters for optimal performance (efficiency)	Thermohydraulic/thermal performance (efficiency)	Comments
						(iii) GA optimized parameters with maximum exergy efficiency of 5.2%. (iv) Optimum values were obtained for design and operating parameters. (v) Results of model simulations for proposed SAH were validated with the models available in the recent literature.
9.	Gholami et al. (2019) [204]	A SAH with arcuate-shaped obstacles	NSGA-II	(i) Range of flow rate (kg s^{-1}): 0.001–0.5 (ii) Inlet temperature range (K): 273.0–300.0 (iii) Inlet temperature range (K): 273.0–410.0 (iv) Range of area (m^2): 1.0–5.0 (v) Solar irradiance (W m^{-2}): 800.0	Exergy efficiency of collectors with obstacles: 3.5%	(i) Their results indicate that both the double glass cover and obstacle (type III) SAHs were more efficient in terms of economic and exergetic characteristics than the alternatives considered in their study.
10.	Yıldırım and Aydoğdu (2017) [23]	Flat plate SAHs: (i) Single-pass SAH (ii) Double-parallel pass SAH	ABC	The optimum channel depth and optimum air mass flow rates were both evaluated for different collector lengths and different solar radiations. Their analysis and comparisons were shown in tables in [23].	The maximum thermohydraulic efficiency: (i) Single-pass SAH: 71.43% (ii) Double-parallel pass SAH: 82.91%	(i) The ABC optimization technique was found to be applicable to optimize the SAHs. (ii) Some design parameters like the channel depth and air mass flow rate can be assessed for optimum thermohydraulic efficiency. (iii) Optimum thermohydraulic efficiency decreased with increasing collector lengths. (iv) Thermal efficiencies corresponding to maximum thermohydraulic efficiencies decreased with increasing collector lengths. (v) The optimum channel depth increased with increasing collector lengths. (vi) Solar insolation increased the heat gain and enhanced both the thermal efficiencies and thermohydraulic performance.
11.	Siddhartha et al. (2012) [210]	Flat plate SAH	SA	(i) Wind velocity: 1.0 m/s (ii) Tilt angle: 70.0° (iii) Irradiance: 600.0 W/m^2 (iv) Plate emissivity: 0.85	The optimized thermal efficiency: 72.48%	(i) The thermal efficiency of a flat plate SAH increases with the Reynolds number. (ii) The thermal efficiency of a flat plate SAH increases with the number of glass cover plates and tilt angle.

TABLE 4: Continued.

| S. no.	Author(s), year(s), and references	Types of SAHs	Metaheuristic algorithm(s)	Important considered input/design/operating parameters for optimal performance (efficiency)	Thermohydraulic/thermal performance (efficiency)	Comments
				(v) Reynolds number: 20,000.0		(iii) Upon comparison with the GA, the empirical SA optimal thermal efficiencies were similar to GA. However, the GA values were higher than SA estimates.
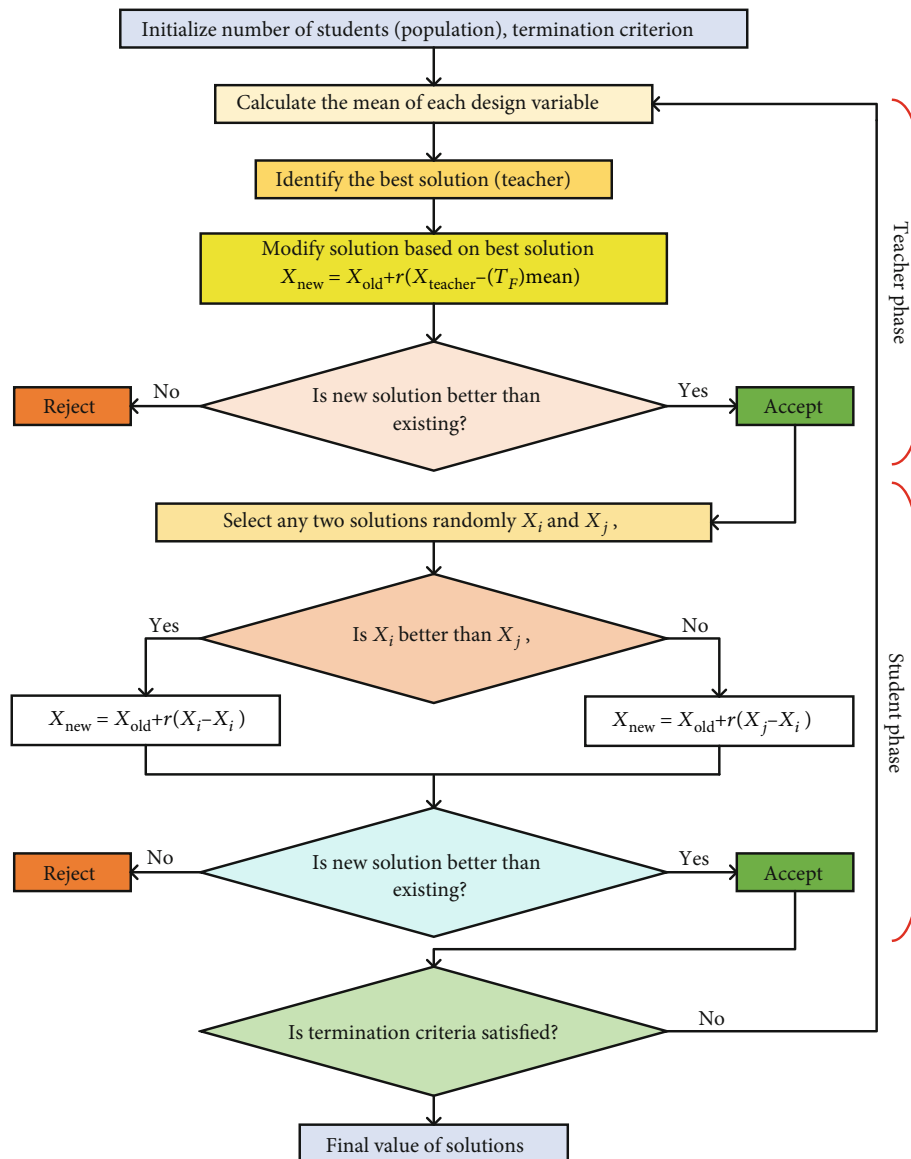
FIGURE 10: Flowchart of the TLBO algorithm based on Rao et al. [195].

optimization algorithms like GA, PSO, and SA applying wide-ranging computational tests on a flat surface SAH. Consequently, the TLBO and ELTBO algorithms were found to be extremely effective. Additionally, the thermal performance increased not only with the Reynolds number but also slightly with the glass cover plates.
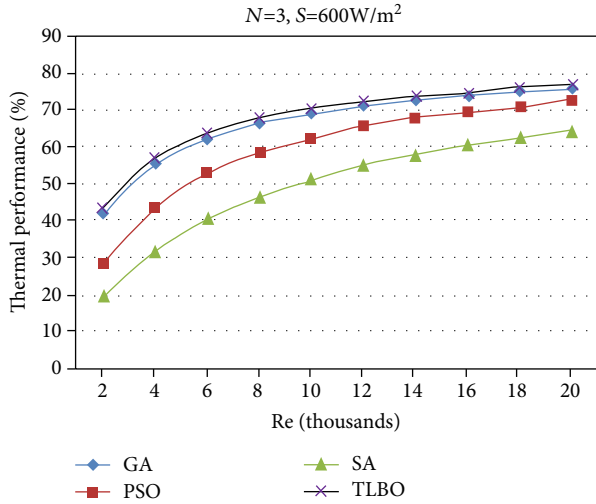
FIGURE 11: Thermal efficiency of metaheuristic algorithms against Reynolds number [24].

4.3. Using the Genetic Algorithm (GA)

4.3.1. Basic Concept of the Genetic Algorithm. The GA is an algorithm based on biology and inspired by the mechanism of evolution in nature. The objective function formulation involves expressing the decision variables which are encoded as chromosomes. The GA follows three main steps: selection, crossover, and mutation, as described in the subsection below [25]. For a better understanding, Figure 12 demonstrates the flowchart of the GA based on Yang et al. [26].

Step 1. *Selection.* At first, solutions are generated randomly, and each solution's fitness is evaluated. Only fitter chromosomes for the next generation are chosen after selection.

Step 2. *Crossover.* Spawn the offspring for the next generation as follows:

$$\text{offspring} = \begin{Bmatrix} \alpha \cdot \text{parent}\,1 + (1-\alpha) \cdot \text{parent}\,2 \\ (1-\alpha) \cdot \text{parent}\,1 + \alpha \cdot \text{parent}\,2 \end{Bmatrix}. \tag{21}$$

Step 3. *Mutation.* Help achieve better offspring, which might have missed the crossover operation. As a user-defined mutation rate, β is used for mutation operation.

$$\text{offspring} = \pm\beta \cdot \text{offspring} + \text{offspring}, \tag{22}$$

where α is the crossover rate and β is the mutation rate.

4.3.2. Genetic Algorithm for the Optimization of Solar Air Heaters. In 2010, Varun and Siddhartha [202] used GA to obtain optimal thermal efficiency of flat surface SAH applying the plate emissivity, tilt angle, Reynolds number, and glass plate number. In the study, a computer program-based optimization problem was developed using MATLAB software. Their result showed that the maximum thermal efficiency was 75.65%. The optimized set of values used to obtain that thermal efficiency includes 2.95 m/s air velocity, 65.33° tilt angle, 0.86 plate emissivity, 296.11 K ambient tem-
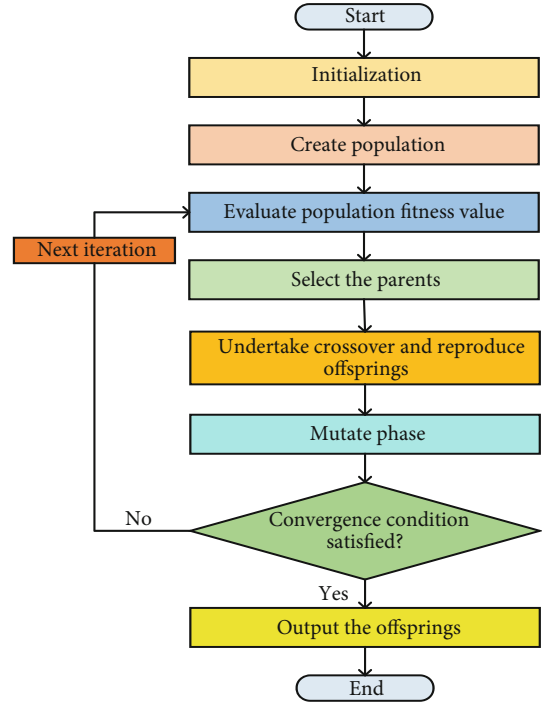

FIGURE 12: Flowchart for the GA method.

perature, and 2.20 K temperature rise. Further, the study showed that the thermal efficiency of a flat plate SAH increased with the Reynolds number. Two years later, Şahin [203] investigated the optimization of a solar air collector (SAC) using the GA and artificial bee colony (ABC) algorithm. The highest optimal thermal efficiency of the SAC emanates from parameter values of the absorber plate emissivity, glass cover emissivity, air temperature, air velocity, and collector slope. Also, the optimal thermal efficiencies of 79.98% and 79.83% were obtained when applying the ABC and GA, respectively. Also, SAC thermal performance increased with an increase in the Reynolds number. The author showed that both the ABC algorithm and the GA were successfully applied in SAC thermal efficiency optimization. However, the ABC algorithm indicates a greater optimal thermal efficiency than GA, as shown in Figure 13 below.

Recently, Saravanakumar et al. [159] employed GA to optimally design fins and stopper arc-shaped rib SAH for exergy efficiency. In their study, the code developed used MATLAB software to solve energy and exergy balance equations. It was shown that the proposed SAH maximum exergy efficiency at optimized conditions was 5.2%. However, the maximum exergy was obtained for 8 fins, 0.2 m baffle length, 0.015 m baffle width, and 0.012 kg/s mass transfer rate. Finally, their model simulations for the proposed SAH were validated with models available in the recent literature. Until now, many evolutionary multiobjective algorithms were derived from GA to optimize different systems. Take the case of SAHs; in Ref. [204], NSGA-II (nondominated sorting genetic algorithm-II) optimized thermoeconomic barrier arcuate-shaped SAHs. Their results indicate that both the double glass cover and barrier (type III) SAHs had the highest economic and exergetic optimization systems in their
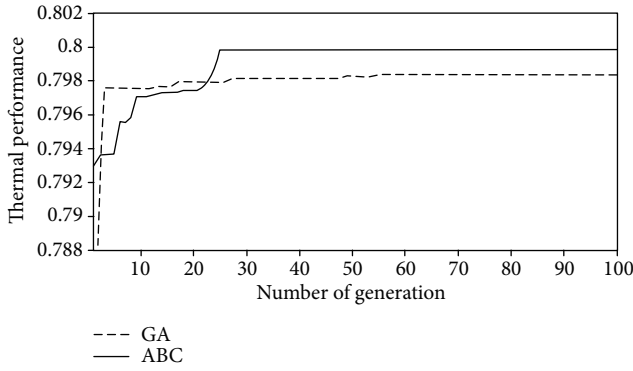
FIGURE 13: ABC and GA results for thermal performance of the study in [203].

study. The optimization parameters and outcome of the study are summarized in Table 4 below.

4.4. Using the Artificial Bee Colony (ABC)

4.4.1. Basic Concept of the Artificial Bee Colony. The ABC algorithm was stimulated through the intelligent feeding nature of honey bees [205]. The ABC algorithm comprises four main stages as described below [205–207]:

(1) Initial Stage. In the initial level, the ABC algorithm produces an arbitrarily dispersed basic population which incorporates SN (food source number equals employed bee number) solution. Considering every food source X_i as a solution trajectory to the optimization problem, every X_i tracks n variables ($X_{ij}, j = 1, \cdots, n$) to minimize the objective function. After initialization, the population of the positions (results) is exposed to replicated periods $C = 1, 2, \cdots, MCN$ (maximum period number). This is the inquiry procedure of the next three phases.

(2) Working Bee Stage. Working bees seek fresh food supply v_{ij} containing greater nectar in the surroundings of the food supply (x_{ij}) in their consciousness. They discover a neighboring food source and assess its expediency (appropriateness). Thus, the nearby food supply is evaluated from the following equation:

$$v_{ij} = x_{ij} + r_{ij} \cdot \left(x_{ij} - x_{kj} \right), \tag{23}$$

where x_{kj} is the arbitrarily preferred food supply, i is the arbitrarily preferred specification indicator $k \neq i$, and r_{ij} is the arbitrary number in the interval $[0, 1]$. After generating the fresh food supply (v_{ij}), its health is evaluated, and a hungry choice is made between v_{ij} and x_{ij}. This appropriate value indicates the working bee's wiggle dance.

(3) Onlooker Bee Stage. Idle bees comprise two groups of bees: bystander bees and recruiters. Working bees share information about their food supply with spectator bees waiting in the hive, and the bystander bees determine their food sources based on this information. The possibility p_i for
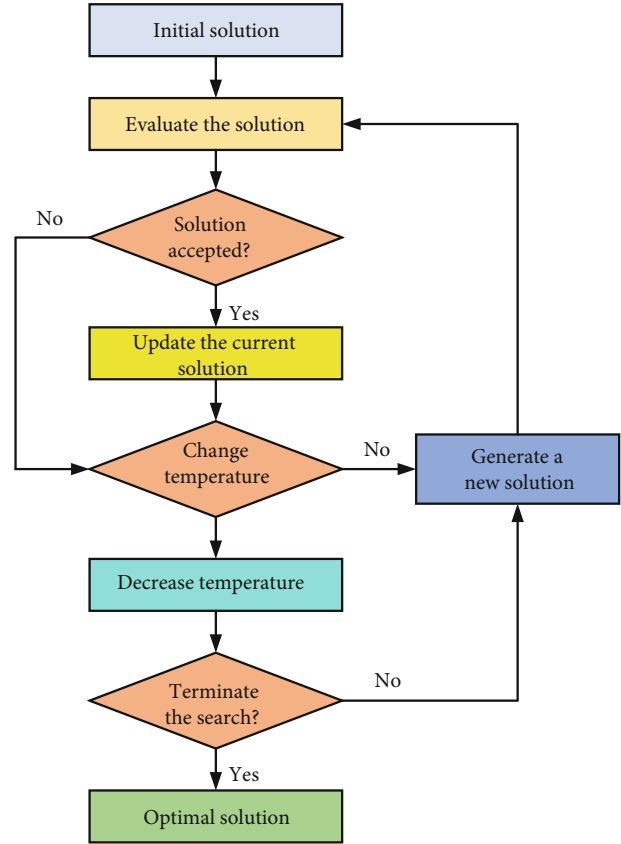

FIGURE 14: Flowchart for optimization using the SA algorithm based on Zain et al. [209].

which x_i is preferred by a spectator bee is evaluated by the equation below:

$$p_i = \frac{\text{fitness}_i(x_i)}{\sum_{i=1}^{n} \text{fitness}_i(x_i)}. \tag{24}$$

After a food supply x_i is selected by chance for a bystander bee, a nearby source v_{ij} is judged utilizing Equation (23), and its appropriate value is estimated. Therefore, more bystanders are enlisted to source for food, and a definite response behavior develops.

(4) Detective Bee Stage. The idle bees which arbitrarily select their food origins are scouts. Working bees, which cannot be enhanced by a fixed number of trials, as indicated by the ABC algorithm, become recruiters, and those poor results must be discarded. Therefore, the transformed scouts arbitrarily seek new solutions, which were uncovered by the scouts that were the working bees of x_i.

4.4.2. Artificial Bee Colony Solar Air Heater Optimization. In 2012, Şahin [203] studied the optimization of SAC using the GA and ABC algorithm. However, the ABC algorithm showed better performance results than GA, as shown in the previous subsection and in Table 4. A recent study by Yıldırım and Aydoğdu [23] developed the ABC algorithm

TABLE 5: Summary of the advantages and disadvantages of six discussed methods in SAH optimization.

S. no.	Algorithm	Advantages	Disadvantages	Remarks
1.	Simulated annealing (SA)	(i) Easy to implement [24] (ii) Converge under appropriate conditions	(i) SA has a lower performance than GA [210] (ii) The SA algorithm is inferior to alternative optimization algorithms like GA, PSO, and TLBO [24] (iii) Slow convergence [28] (iv) SA is not suitable for working at some temperature and irradiance values [28]	Although SA was tried for the optimization of SAHs, the present literature has shown that it is inferior to the alternative optimization algorithms like GA, PSO, and TLBO.
2.	Particle swarm optimization (PSO)	(i) PSO considers different and better positions to update the population (ii) Simple in concept (iii) Higher convergence speed [14] (iv) Easy to be implemented [14]	(i) In Ref. [84], PSO methodology did not show better optimization compared to TLBO (ii) PSO depends on the inertial weight and learning constants [213]	PSO works well for determining the maximum optimal thermal efficiency of SAHs. However, there are other algorithms that work better than PSO.
3.	Genetic algorithm (GA)	(i) Accurate and quick compared to traditional methods [203]	(i) In [202], the thermal efficiency of SAH was reported to be very poor. This was due to its low heat transfer capability, and it depends upon the various system and operating parameters (ii) Generally, GA tends to be trapped into local minima (iii) Difficult to converge (iv) It can produce meaningless results	GA remains one of the most widely used optimization algorithms. According to the literature on SAH optimization, it still shows that some drawbacks like poor thermal efficiency exist.
4.	Artificial bee colony (ABC)	(i) Accurate and quick compared to traditional methods [203] (ii) In Ref. [203], the thermal efficiency of SAC obtained by the ABC algorithm was slightly higher than the thermal efficiency obtained by GA (iii) Simple as the PSO algorithm, but with fewer restriction limits like the highest cycle count and colony extent [214]	(i) Some parameters can affect the algorithm efficiency [23] (ii) Slow convergence speed [212]	According to the recent literature, despite some drawbacks, ABC has shown good results for the optimization of SAHs.
5.	Teaching-learning-based optimization (TLBO)	(i) In Ref. [24], TLBO was found to be more acceptable than alternative optimization algorithms like GA, PSO, and SA (ii) It is an efficient algorithm [24] (iii) It is a promising algorithm for determining optimal designs [24] (iv) In Ref. [84], the TLBO approach showed better results for maximizing the efficiency than the PSO technique (v) It is a simple and low-cost method in terms of metaheuristic evaluation for thermohydraulic efficiency of roughened SAHs [84] (vi) A fast convergence speed [215] (vii) A high precision algorithm [215]	(i) The TLBO only requires tuning of the algorithm's accepted regulating limits for its operation [201]	Until now, TLBO has shown good results for the optimization of SAHs compared to the other optimization methods.
6.	Elitist teaching-learning-based optimization (ETLBO)	(i) In Ref. [200], ETLBO and TLBO algorithms were both found to be more acceptable than alternative optimization algorithms like GA, PSO, and SA (ii) It is an efficient algorithm [200]	(i) The impact of the ETLBO algorithm's accepted governing metrics like the population size, generation number, and elite size on the algorithm's efficiency must be considered and investigated in detail.	According to the recent literature, both the ETLBO and TLBO algorithms perform better than the other optimization algorithms considered by the previous researchers. Until recently, despite

TABLE 5: Continued.

S. no.	Algorithm	Advantages	Disadvantages	Remarks
		(iii) It is a promising algorithm for determining optimal designs [200]	But, the TLBO only requires tuning of the algorithm's accepted supervising limits for its operation [201]	the mentioned drawbacks of this approach, there are not many research papers on SAH optimization applying this algorithm.

simulation code based on models written in MATLAB software to optimize flat plate SAHs. They obtained the operating values and optimum design using the algorithm with different insolation values and collector lengths. The obtained maximum thermohydraulic performances of single-pass SAH and double-parallel pass SAH were 71.43% and 82.91%, respectively. The authors also showed that using some design parameters like the channel depth and air mass flow rate, the ABC optimization technique can also be used to optimize flat plate SAHs.

4.5. Using the Simulated Annealing Algorithm (SA)

4.5.1. Basic Concept of the Simulated Annealing Algorithm. The SA algorithm was first used for a solution of the traveling salesman problem by Kirkpatrick et al. in 1983 [208]. It was inspired by the physical gradual cooling process called annealing [26]. The SA technique uses two main processes: (1) changeover between states and (2) temperature control to achieve the minimum energy level. The SA procedure begins at an initial stable position "X_i" of the energy stratum "E_i." Then, the following condition "X_2" of the energy stratum "E_2" is admissible only if the expression below is fulfilled [25]:

$$E_1 - E_2 \leq 0. \tag{25}$$

If $E_1 - E_2 > 0$, the state is shown by the following equation [25]:

$$P(E, T_C) = e^{(E_1 - E_2)/K_B T_C}. \tag{26}$$

The control parameter "T_C" is regulated during the whole algorithm search procedure until the minimum energy level is obtained. Figure 14 below shows the optimal algorithmic solution of the simulated annealing approach.

4.5.2. Simulated Annealing Optimization Algorithm of Solar Air Heaters. In 2012, a comparative study by Siddhartha et al. [210] assessed the thermal efficiency optimization of smooth flat surface SAH and forecasted the optimized design of SA. In the study, the algorithm for optimization was developed and simulation was conducted based on the code developed in MATLAB software. The results showed that the optimized thermal performance was 72.48% using $600.0 \, \text{W/m}^2$ irradiance and three glass plates. In addition, these results were then compared with those given by other metaheuristic algorithms like GA and PSO and found satisfactory. Comparisons between the closest empirical data and the thermal efficiency of SA were very close to the GA results. However, the GA values were higher than those of SA.

Few years later, Rao and Waghmare [24] evaluated the thermal efficiency optimization of smooth flat surface SAH applying the TLBO technique and then compared the results with those given by other metaheuristic techniques like SA, PSO, and GA from the previous literature. This study was well discussed in the previous subsection. The SA algorithm is useful for the optimal thermal efficiency of smooth flat plate SAH. However, the SA technique was not the most powerful thermal efficiency optimization algorithm for the smooth flat plate SAH, as shown in Figure 11 above.

5. Discussion

At present, fossil fuels, including natural gas, oil, and coal, are the main primary world energy sources. Due to the finite size of fossil fuel reserves, a big energy dilemma in this century is "when will fossil fuels run out?" That is a pivotal and controversial question that needs to be addressed. An interesting study published in 2009 by Shafiee and Topal [211] proposed a method for largely calculating when fossil fuels are to be depleted. The predominant external characteristics affecting oil, coal, and gas reserve trends in the econometric models were their consumption and price rates between 1980 and 2006, respectively. The results from the proposed method showed that the depletion times of fossil fuels were estimated at around 35, 37, and 107 years for oil, gas, and coal, respectively. Accordingly, this means that only coal will still be available after 2042 and up to 2112 if consumption is at conservative rates.

Certainly, in a few decades, renewable energy should be continuing to rise, edging out fossil fuels, and lowering greenhouse gas emissions. This sustainable renewable energy outlook will be critical to expanding energy access for all, reducing air pollution, and tackling greenhouse gas emissions. Expanding renewable energy use and energy efficiency measures can considerably sustain energy use by reducing the cooling and heating demand. SAHs can, therefore, be a part of the other promising renewable energy systems to reduce carbon dioxide emissions in the next decades. SAHs have abundant benefits, like small manufacturing, equipment, and operating expense, and may be built by applying less and cheaper materials. Nevertheless, the performance of SAHs was criticized for being poor, and researchers and developers are exerting great efforts to improve their thermal performance indices. The low efficiency of SAHs can be enhanced using heat storage materials, appropriate absorber coatings, packed beds, fins, or corrugated surfaces, as discussed in Section 3.4.4.

TABLE 6: The very recent papers on the existing methods and techniques used by other researchers in the optimization of solar air heaters (2019-2021).

S. no.	Authors, year, and references	Objective of the study	Methods/techniques	Concluding important remarks
1.	Zhu and Zhang (2020) [216]	A numerical investigation on performance optimization of a microheat pipe array-based SAH	(i) A three-dimensional steady-state numerical model using CFD software (ii) Experimental system was built and used to verify the numerical model	The developed numerical model was validated in agreement with the experimental results.
2.	Benhamza et al. (2021) [217]	Exergy, energy, and improvement potential-dependent food drying multiobjective design optimization SAH	(i) Experimental configuration (ii) Response surface methodology (RSM) model (iii) Mathematical model	An energy balance equation SAH numerical model was developed and also empirically validated. The 5.745% mean applicable error indicates that both the analytical and empirical results of the algorithm are similar. Moreover, the analysis of variance proved that the response surface methodology (RSM) regression models were very precise. As a result, they may be applied to SAH optimization.
3.	Korpale et al. (2020) [218]	Numerical simulations and optimization of SAHs	(i) Empirical correlations and evaluation of maximum thermohydraulic efficiency of rectangular section ribs installed in SAHs (ii) CFD simulations (iii) Experimental	The errors were within acceptable limits, proving that the accuracy of empirical correlations used for the design of SAHs and proper selection of model equations were adequate.
4.	Kumar et al. (2020) [85]	The thermohydraulic optimization of SAH with packed bed duct	(i) In this investigation, the heat exchange and fluid flow SAH features were numerically analyzed to obtain optimal performance	The study concluded that there was a slight enhancement reduction with temperature rise for every set of the bed depth to packing element size ratios.
5.	Sharma and Choudhary (2020), chapter 6 in Ref. [219]	A multiobjective performance optimization of a ribbed SAH	(i) CFD-Taguchi approach	Their efficient heat exchange application investigation appropriately offered an improved rib design.
6.	Bezbaruah et al. (2019) [220]	The truncated half-conical vortex generator SAH optimization using both general efficiency analysis and grey comparative analysis (GRA)	(i) Numerical method (ii) Grey relational analysis (GRA) optimization	They applied the disparate curves from the CFD code to confirm their results.
7.	Dezan et al. (2020) [98]	A thermohydraulic efficiency SAH duct optimization using irregular rectangular winglet row pairs	(i) Proxy optimization (ii) Multiobjective optimization (iii) Numerical method	They apply to sustainable optimal channel-type SAHs.
8.	Xiao et al. (2019) [221]	Exergy destruction minimization-dependent turbulent heat exchange SAH optimization.	(i) Heat exchange optimization	Their results showed that the optimization technique was efficient for enhancing the SAH thermohydraulic efficiency.
9.	Qader et al. (2019) [222]	Modeling of inclined fin optimization design SAH.	(i) Response surface methodology (RSM) (ii) Simulation using ANSYS FLUENT v16.1 software	The thermal efficiency of the inclined fin SAH was better and more distinguished than the circle, square-sectioned, and L-shaped coarse SAH geometries.
10.	Kumar et al. (2019) [223]	The efficiency assessment and discrete multiple arc-shaped rib SAH optimization	(i) Response surface methodology (RSM) (ii) Analysis of variance (ANOVA) (iii) Experimental	An extraordinary enhancement in the thermal efficiency of SAH varied with coarseness but led to higher SAH pumping power.
11.	Debnath et al. (2019) [224]	Integrated fuzzy method model for flat plate SAC optimization.	(i) Experimental (ii) Integrated fuzzy method	The accuracy of the obtained result for the SAC was found to be about 97.5%.

Currently, SAH optimization is used to curtail the total system cost, increase life cycle savings, and enhance thermal efficiency. To meet the energy demands, it is necessary to make optimal use of solar resources. To achieve this goal, a wide range of optimization techniques can be implemented, either deterministic or stochastic. Furthermore, using metaheuristic algorithms, we obtain the optimum design for maximum SAH efficiencies. The aim of this article is to undertake a detailed survey of six promising metaheuristic algorithms and their application in SAH optimization. Studies [14, 23, 24, 84, 159, 194, 200, 202–204, 210] from Table 4 below show that metaheuristic algorithms are particularly effective and powerful tools for finding optimal performance efficiencies of SAHs. Moreover, Table 5 illustrates the main advantages and disadvantages of these six metaheuristic algorithms. Undeniably, these capabilities and demerits from Table 5 can provide potential insight into future research on SAH optimization.

Kumar and Layek [84] used two metaheuristic algorithms (PSO and TLBO) to optimize the performance of roughened SAHs. As shown in Figure 9 and Tables 4 and 5, the TLBO approach outperformed the PSO technique.

A comparative study by Şahin [203] evaluated the optimization of SAC using the GA and ABC algorithm. The results indicate that ABC and GA were successfully applied to the thermal performance optimization of SAC. However, the ABC algorithm showed better results than GA (see Table 4 below). However, studies in [23, 212] reported some drawbacks of this technique as some parameters can affect the algorithm performance and the low convergent speed (see Table 5 below). Siddhartha et al. [210] studied the thermal efficiency optimization of smooth flat surface SAH, optimized the design using SA, and then correlated it with alternative metaheuristic algorithms like GA and PSO. This comparison showed that the thermal efficiency was very close. However, the GA values were higher than SA estimates. Rao and Waghmare [24] and Rao [200] studied the efficiency of a smooth flat surface SAH applying ETLBO and TLBO algorithms and then correlated the results with alternative optimization algorithms like SA, PSO, and GA. The comparison showed that TLBO and ELTBO algorithms were more effective than SA, PSO, and GA, as shown in Figure 11. Also, the thermal efficiency increases with the Reynolds number.

From the recent literature and the comparison summary in Tables 4 and 5, metaheuristic algorithms like ETLBO, TLBO, ABC, GA, PSO, and SA generate better results for SAH optimization. However, TLBO is more competitive than ABC, GA, PSO, and SA for the optimization of SAHs for the same considered problem. Although the metaheuristic algorithms have shown the capability of the optimization of SAHs, there are also other ways to optimize these solar systems. As an illustration, Table 6 summarizes the very recent papers on the existing methods and techniques used by other researchers in the optimization of SAHs.

6. Conclusions and Future Outlook

The present paper reviews the recent studies on the applications of six state-of-the-art metaheuristic algorithms in solar air heater optimization and highlights their recent trends and future prospects. Such algorithms include simulated annealing (SA), particle swarm optimization (PSO), genetic algorithm (GA), artificial bee colony (ABC), teaching-learning-based optimization (TLBO), and elitist teaching-learning-based optimization (ETLBO). It is clearly indicated from the review that the use of metaheuristic algorithms results in achieving significant improvements in the efficiency of solar air heaters. The discussion reviewed six metaheuristic techniques used either individually or in combination to give better results than experimental findings. Until recently, these optimization techniques have never been widely employed in SAH optimization. However, in only one work for SA and GA comparison [210], the GA was reported to have higher values than SA. Also, SA was reported to have results that are closer to experimental results when compared to GA. In the literature, studies reported TLBO to be competitive with the other methods. In this case, studies in Ref. [24, 84, 199] compared TLBO, PSO, SA, and GA. All their solutions indicate that the TLBO method is superior to the alternative optimization algorithms in the new literature. In only one work [203], both GA and ABC were used to maximize SAH. The ABC algorithm showed superior results than GA. However, there are also some drawbacks of this optimization method, as shown in Table 5.

For a thorough analysis of the comparison summary, see Tables 4 and 5 and Figures 9, 11, and 13 for the already published literature. It is clear that the metaheuristic algorithms such as ETLBO, TLBO, ABC, GA, PSO, and SA generate better results than the conventional SAH optimization. However, both ETLBO and TLBO are more efficient than ABC, GA, PSO, and SA in the optimization of SAHs for the same considered problem.

In solar air heater optimization, there can also be enough opportunity for deploying various metaheuristic enhanced SAHs. Furthermore, the study can be extended to perform thermal performance optimization for solar air heaters. The following references show specific published papers on the use of metaheuristic algorithms in SAH optimization: [202] in 2010, [14] in 2012, [210] in 2012, [203] in 2012, [24] in 2015, [200] in 2016, [23] in 2017, [84, 204] in 2019, and [159, 194] in 2020. Hence, it can be observed that the total number of publications on this topic has increased slightly since 2010 (even though information for 2020 is not yet complete at the moment). Although ETLBO and TLBO are undoubtedly more competitive than ABC, GA, PSO, and SA in the literature, it is difficult to declare one of these techniques as the best for optimization of SAHs. This is so because there are yet a few works on this topic, and all of the reviewed techniques have been reported as successful methods of optimization of SAHs, as shown in Table 4.

To our knowledge, there are many types of metaheuristic techniques that have not yet been utilized for SAH optimization. These optimization techniques include the differential evolution, cuckoo search, grey wolf optimization, flower pollination algorithm, and whale optimization algorithm. In brief, we recommend all twenty-eight metaheuristic algorithms (found in [26]) that have already been applied on PV cell parameter identification to be used in SAH

optimization. These recommended optimization methods, as well as those to be introduced in the future, are expected to be applied in further research and studies to produce the best thermal efficiencies for the various SAHs.

Nomenclature

$\dot{E}x$:	Exergy rate (W)
$\dot{E}x_{dest}$:	Rate of exergy destruction (W)
$\dot{Q}_c$:	Energy incident on the evacuated cube
$\dot{Q}_f$:	Energy absorbed by air (W)
$\dot{Q}_u$:	Useful energy gained from the collector
A_c:	Absorber plate area (m^2)
C_p:	Specific heat of air (J kg^{-1} K^{-1})
$\dot{E}$:	Energy rate (W)
K_B:	Boltzmann constant
$\dot{m}$:	Mass flow rate of air (kg/s)
ΔT:	Temperature difference (°K)
h:	Enthalpy (J/kg)
PJ:	Petajoule
Re:	Reynolds number
T:	Temperature (°C)
I:	Intensity of solar radiation at a particular area (W/m^2)
P:	Fluid pressure (Pa)
R:	Correlation coefficient
s:	Specific entropy
ANSYS:	Mechanical finite element analysis *software* is used to simulate computer models of structures, electronics, or machine components for analyzing strength, toughness, elasticity, temperature distribution, electromagnetism, fluid flow, and other attributes.

Abbreviations

ABC:	Artificial bee colony
ANOVA:	Analysis of variance
ASHRAE:	American Society of Heating, Refrigerating and Air-Conditioning Engineers
CFD:	Computational fluid dynamics
DE:	Differential evolution
ETLBO:	Elitist teaching-learning-based optimization
GA:	Genetic algorithm
GRA:	Grey relational analysis
MATLAB:	Matrix laboratory
MIT:	Massachusetts Institute of Technology
MOPSO:	Multiobjective particle swarm optimization
NSGA-II:	Nondominated sorting genetic algorithm-II
PCM:	Phase change materials
PSO:	Particle swarm optimization
PV:	Photovoltaic
PV/T:	Photovoltaic/thermal
QPSAC:	Quadruple-pass solar air collector
RNG:	Renormalization group
RSM:	Response surface methodology
SA:	Simulated annealing
SAC:	Solar air collector

SAH(s):	Solar air heater(s)
SIMPLE:	Semi-implicit pressure-linked equation (an algorithm)
SST:	Shear stress transport
SWH(s):	Solar water heater(s)
TES:	Thermal energy storage
TLBO:	Teaching-learning-based optimization
N/A:	Not available.

Greek Symbols

η_{II}:	Exergy efficiency
α:	Absorptance of the inner surface of the evacuated tube collector
η:	Thermal efficiency
τ:	Transmittance of the collector tube
ψ:	Specific exergy.

Subscripts

2D:	Two-dimensional
3D:	Three-dimensional
a:	Ambient air
c:	Collector
f:	Fluid
fi:	Inlet air
fm:	Mean air
fo:	Outlet air
in/i:	Input
out/o:	Output
p:	Plate.

Conflicts of Interest

The authors declare no conflict of interest.

Authors' Contributions

The authors contributed equally to the completion of this paper.

Acknowledgments

References

[1] N. Kannan and D. Vakeesan, "Solar energy for future world: - a review," *Renewable and Sustainable Energy Reviews*, vol. 62, pp. 1092–1105, 2016.

[2] X. Han, X. Chen, M. B. McElroy, S. Liao, C. P. Nielsen, and J. Wen, "Modeling formulation and validation for accelerated simulation and flexibility assessment on large scale power systems under higher renewable penetrations," *Applied Energy*, vol. 237, pp. 145–154, 2019.

[3] M. Benasla, D. Hess, T. Allaoui, M. Brahami, and M. Denaï, "The transition towards a sustainable energy system in Europe: what role can North Africa's solar resources play?," *Energy Strategy Reviews*, vol. 24, pp. 1–13, 2019.

[4] A. Modi, F. Bühler, J. G. Andreasen, and F. Haglind, "A review of solar energy based heat and power generation systems," *Renewable and Sustainable Energy Reviews*, vol. 67, pp. 1047–1064, 2017.

[5] E. Kabir, P. Kumar, S. Kumar, A. A. Adelodun, and K. H. Kim, "Solar energy: potential and future prospects," *Renewable and Sustainable Energy Reviews*, vol. 82, pp. 894–900, 2018.

[6] A. Shahsavari and M. Akbari, "Potential of solar energy in developing countries for reducing energy-related emissions," *Renewable and Sustainable Energy Reviews*, vol. 90, pp. 275–291, 2018.

[7] R. R. Hernandez, S. B. Easter, M. L. Murphy-Mariscal et al., "Environmental impacts of utility-scale solar energy," *Renewable and Sustainable Energy Reviews*, vol. 29, pp. 766–779, 2014.

[8] A. H. Almasoud and H. M. Gandayh, "Future of solar energy in Saudi Arabia," *Journal of King Saud University - Engineering Sciences*, vol. 27, no. 2, pp. 153–157, 2015.

[9] P. G. V. Sampaio and M. O. A. González, "Photovoltaic solar energy: conceptual framework," *Renewable and Sustainable Energy Reviews*, vol. 74, pp. 590–601, 2017.

[10] G. Raina and S. Sinha, "Outlook on the Indian scenario of solar energy strategies: policies and challenges," *Energy Strategy Reviews*, vol. 24, pp. 331–341, 2019.

[11] C. G. Ozoegwu, C. A. Mgbemene, and P. A. Ozor, "The status of solar energy integration and policy in Nigeria," *Renewable and Sustainable Energy Reviews*, vol. 70, pp. 457–471, 2017.

[12] J. D. D. Niyonteze, F. Zou, G. Norense Osarumwense, S. B. Asemota, and G. Shyirambere, "Key technology development needs and applicability analysis of renewable energy hybrid technologies in off-grid areas for the Rwanda power sector," *Heliyon*, vol. 6, no. 1, 2020.

[13] S. Bimenyimana, G. N. O. Asemota, J. D. D. Niyonteze, C. Nsengimana, P. J. Ihirwe, and L. Li, "Photovoltaic solar technologies: solution to affordable, sustainable, and reliable energy access for all in Rwanda," *International Journal of Photoenergy*, vol. 2019, Article ID 5984206, 29 pages, 2019.

[14] Siddhartha, N. Sharma, and Varun, "A particle swarm optimization algorithm for optimization of thermal performance of a smooth flat plate solar air heater," *Energy*, vol. 38, no. 1, pp. 406–413, 2012.

[15] A. Bekele, M. Mishra, and S. Dutta, "Effects of delta-shaped obstacles on the thermal performance of solar air heater," *Advances in Mechanical Engineering*, vol. 3, 2011.

[16] H. S. Arunkumar, K. Vasudeva Karanth, and S. Kumar, "Review on the design modifications of a solar air heater for improvement in the thermal performance," *Sustainable Energy Technologies and Assessments*, vol. 39, p. 100685, 2020.

[17] G. Kalaiarasi, R. Velraj, M. N. Vanjeswaran, and N. Ganesh Pandian, "Experimental analysis and comparison of flat plate solar air heater with and without integrated sensible heat storage," *Renewable Energy*, vol. 150, pp. 255–265, 2020.

[18] T. Alam and M. H. Kim, "A critical review on artificial roughness provided in rectangular solar air heater duct," *Renewable and Sustainable Energy Reviews*, vol. 69, pp. 387–400, 2017.

[19] M. Yang, X. Yang, X. Li, Z. Wang, and P. Wang, "Design and optimization of a solar air heater with offset strip fin absorber plate," *Applied Energy*, vol. 113, pp. 1349–1362, 2014.

[20] A. Kumar and M. H. Kim, "Numerical optimization of solar air heaters having different types of roughness shapes on the heated plate - technical note," *Energy*, vol. 72, pp. 731–738, 2014.

[21] M. Ansari and M. Bazargan, "Optimization of flat plate solar air heaters with ribbed surfaces," *Applied Thermal Engineering*, vol. 136, pp. 356–363, 2018.

[22] A. H. Elsheikh and M. Abd Elaziz, "Review on applications of particle swarm optimization in solar energy systems," *International Journal of Environmental Science and Technology*, vol. 16, no. 2, pp. 1159–1170, 2019.

[23] C. Yıldırım and İ. Aydoğdu, "Artificial bee colony algorithm for thermohydraulic optimization of flat plate solar air heaters," *Journal of Mechanical Science and Technology*, vol. 31, no. 7, pp. 3593–3602, 2017.

[24] R. V. Rao and G. Waghmare, "Optimization of thermal performance of a smooth flat-plate solar air heater using teaching–learning-based optimization algorithm," *Cogent Engineering*, vol. 2, no. 1, p. 997421, 2015.

[25] D. S. Pillai and N. Rajasekar, "Metaheuristic algorithms for PV parameter identification: a comprehensive review with an application to threshold setting for fault detection in PV systems," *Renewable and Sustainable Energy Reviews*, vol. 82, pp. 3503–3525, 2018.

[26] B. Yang, J. Wang, X. Zhang et al., "Comprehensive overview of meta-heuristic algorithm applications on PV cell parameter identification," *Energy Conversion and Management*, vol. 208, p. 112595, 2020.

[27] D. M. Fébba, E. C. Bortoni, A. F. Oliveira, and R. M. Rubinger, "The effects of noises on metaheuristic algorithms applied to the PV parameter extraction problem," *Solar Energy*, vol. 201, pp. 420–436, 2020.

[28] D. Oliva, M. A. Elaziz, A. H. Elsheikh, and A. A. Ewees, "A review on meta-heuristics methods for estimating parameters of solar cells," *Journal of Power Sources*, vol. 435, p. 126683, 2019.

[29] M. Louazani, A. Khouya, K. Amechnoue, A. Gandelli, M. Mussetta, and A. Craciunescu, "Metaheuristic algorithm for photovoltaic parameters: comparative study and prediction with a firefly algorithm," *Applied Sciences*, vol. 8, no. 3, p. 339, 2018.

[30] F. Daniels, J. A. Duffie, and S. F. Singer, "Solar energy research," *Physics Today*, vol. 9, no. 5, pp. 30–30, 1956.

[31] S. F. Singer, "Proceedings of the World Symposium on Applied Solar Energy," *Physics Today*, vol. 9, no. 8, p. 42, 1956.

[32] A. Saxena and A. A. E.-S. Varun, "A thermodynamic review of solar air heaters," *Renewable and Sustainable Energy Reviews*, vol. 43, pp. 863–890, 2015.

[33] R. Moore, *Solar Air Heating and Cooling*, ISS Institute Inc, Camberwell, Australia, 2005.

[34] W. A. B. J. A. Duffie and W. A. Beckman, *Solar Engineering of Thermal Processes, Fourth Edition*, 2013, https://www.wiley.com/en-us/Solar+Engineering+of+Thermal+Processes%2C+4th+Edition-p-9780470873663.

[35] J. F. Kreider, *Handbook of Heating, Ventilation, and Air Conditioning*, CRC Press, 2000.

[36] W. Weiss, J. Suter, and T. Letz, "Comparison of system designs of solar combisystems," in *Proceedings ISES Solar World Congress*, Göteborg, Sweden, 2003.

[37] H. K. Ghritlahre, P. Chandrakar, and A. Ahmad, "A comprehensive review on performance prediction of solar air heaters using artificial neural network," *Annals of Data Science*, pp. 1–45, 2019.

[38] N. Nader, W. Al-Kouz, and S. Al-Dahidi, "Assessment of existing photovoltaic system with cooling and cleaning system: case study at Al-Khobar city," *Processes*, vol. 8, no. 1, 2020.

[39] R. K. Akikur, R. Saidur, H. W. Ping, and K. R. Ullah, "Comparative study of stand-alone and hybrid solar energy systems suitable for off-grid rural electrification: a review," *Renewable and Sustainable Energy Reviews*, vol. 27, pp. 738–752, 2013.

[40] C. O. C. Oko, E. O. Diemuodeke, N. F. Omunakwe, and E. Nnamdi, "Design and economic analysis of a photovoltaic system: a case study," *International Journal of Renewable Energy Development*, vol. 1, no. 3, pp. 65––673, 2012.

[41] Y. Qiu, Y. D. Wang, and J. Wang, "Soak up the sun: impact of solar energy systems on residential home values in Arizona," *Energy Economics*, vol. 66, pp. 328–336, 2017.

[42] M. S. Cengiz and M. S. Mamiş, "Price-efficiency relationship for photovoltaic systems on a global basis," *International Journal of Photoenergy*, vol. 2015, Article ID 256101, 12 pages, 2015.

[43] C. A. Hossain, N. Chowdhury, M. Longo, and W. Yaïci, "System and cost analysis of stand-alone solar home system applied to a developing country," *Sustainability*, vol. 11, no. 5, p. 1403, 2019.

[44] A. Sreekumar, "Techno-economic analysis of a roof-integrated solar air heating system for drying fruit and vegetables," *Energy Conversion and Management*, vol. 51, no. 11, pp. 2230–2238, 2010.

[45] V. Tomar, G. N. Tiwari, and B. Norton, "Solar dryers for tropical food preservation: thermophysics of crops, systems and components," *Solar Energy*, vol. 154, pp. 2–13, 2017.

[46] S. Shamekhi-Amiri, T. B. Gorji, M. Gorji-Bandpy, and M. Jahanshahi, "Drying behaviour of lemon balm leaves in an indirect double-pass packed bed forced convection solar dryer system," *Case Studies in Thermal Engineering*, vol. 12, pp. 677–686, 2018.

[47] A. D. Tuncer, A. Sözen, A. Khanlari, A. Amini, and C. Şirin, "Thermal performance analysis of a quadruple-pass solar air collector assisted pilot-scale greenhouse dryer," *Solar Energy*, vol. 203, pp. 304–316, 2020.

[48] A. H. A. Al-Waeli, K. Sopian, H. A. Kazem, and M. T. Chaichan, "Photovoltaic/thermal (PV/T) systems: status and future prospects," *Renewable and Sustainable Energy Reviews*, vol. 77, pp. 109–130, 2017.

[49] Y. Jia, G. Alva, and G. Fang, "Development and applications of photovoltaic–thermal systems: a review," *Renewable and Sustainable Energy Reviews*, vol. 102, pp. 249–265, 2019.

[50] T. M. Sathe and A. S. Dhoble, "A review on recent advancements in photovoltaic thermal techniques," *Renewable and Sustainable Energy Reviews*, vol. 76, pp. 645–672, 2017.

[51] S. R. Abdallah, H. Saidani-Scott, and O. E. Abdellatif, "Performance analysis for hybrid PV/T system using low concentration MWCNT (water-based) nanofluid," *Solar Energy*, vol. 181, pp. 108–115, 2019.

[52] A. H. A. Al-Waeli, K. Sopian, M. T. Chaichan et al., "Evaluation of the nanofluid and nano-PCM based photovoltaic thermal (PVT) system: an experimental study," *Energy Conversion and Management*, vol. 151, pp. 693–708, 2017.

[53] S. Aberoumand, S. Ghamari, and B. Shabani, "Energy and exergy analysis of a photovoltaic thermal (PV/T) system using nanofluids: an experimental study," *Solar Energy*, vol. 165, pp. 167–177, 2018.

[54] Y. Hu, P. K. Heiselberg, H. Johra, and R. Guo, "Experimental and numerical study of a PCM solar air heat exchanger and its ventilation preheating effectiveness," *Renewable Energy*, vol. 145, pp. 106–115, 2020.

[55] Y. Zhang, Z. Liu, Z. Wu, L. Zhang, and Y. Luo, "Numerical evaluation on energy saving potential of the photovoltaic fresh air preheating system in different climate regions of China," *Applied Thermal Engineering*, vol. 154, pp. 407–418, 2019.

[56] A. Uzun, B. Bokor, and D. Eryener, "PEM fuel cell performance with solar air preheating," *International Journal of Hydrogen Energy*, vol. 45, no. 60, pp. 34654–34665, 2020.

[57] W. R. Tyfour, G. Tashtoush, and A. Al-Khayyat, "Design and testing of a ready-to-use standalone hot air space heating system," *Energy Procedia*, vol. 74, pp. 1228–1238, 2015.

[58] A. Al-damook and W. H. Khalil, "Experimental evaluation of an unglazed solar air collector for building space heating in Iraq," *Renewable Energy*, vol. 112, pp. 498–509, 2017.

[59] S. Ran, X. Li, W. Xu, and B. Wang, "A solar-air hybrid source heat pump for space heating and domestic hot water," *Solar Energy*, vol. 199, pp. 347–359, 2020.

[60] D. N. Nkwetta and J. Sandercock, "A state-of-the-art review of solar air-conditioning systems," *Renewable and Sustainable Energy Reviews*, vol. 60, pp. 1351–1366, 2016.

[61] A. Allouhi, T. Kousksou, A. Jamil, T. El Rhafiki, Y. Mourad, and Y. Zeraouli, "Economic and environmental assessment of solar air-conditioning systems in Morocco," *Renewable and Sustainable Energy Reviews*, vol. 50, pp. 770–781, 2015.

[62] J. Dardouch, M. Charia, and A. Bernatchou, "Modeling and simulation of absorption solar air conditioning in Morocco

weather conditions," *Materials Today: Proceedings*, vol. 27, pp. 3217–3223, 2020.

[63] M. De Rosa, V. Bianco, F. Scarpa, and L. A. Tagliafico, "Heating and cooling building energy demand evaluation; a simplified model and a modified degree days approach," *Applied Energy*, vol. 128, pp. 217–229, 2014.

[64] M. Isaac and D. P. van Vuuren, "Modeling global residential sector energy demand for heating and air conditioning in the context of climate change," *Energy Policy*, vol. 37, no. 2, pp. 507–521, 2009.

[65] J. L. Reyna and M. V. Chester, "Energy efficiency to reduce residential electricity and natural gas use under climate change," *Nature Communications*, vol. 8, no. 1, 2017.

[66] K. Rajarajeswari and A. Sreekumar, "Matrix solar air heaters – a review," *Renewable and Sustainable Energy Reviews*, vol. 57, pp. 704–712, 2016.

[67] V. V. Tyagi, N. L. Panwar, N. A. Rahim, and R. Kothari, "Review on solar air heating system with and without thermal energy storage system," *Renewable and Sustainable Energy Reviews*, vol. 16, no. 4, pp. 2289–2303, 2012.

[68] H. F. Oztop, F. Bayrak, and A. Hepbasli, "Energetic and exergetic aspects of solar air heating (solar collector) systems," *Renewable and Sustainable Energy Reviews*, vol. 21, no. 215, pp. 59–83, 2013.

[69] V. V. Tyagi, A. K. Pandey, G. Giridhar, B. Bandyopadhyay, S. R. Park, and S. K. Tyagi, "Comparative study based on exergy analysis of solar air heater collector using thermal energy storage," *International Journal of Energy Research*, vol. 36, no. 6, pp. 724–736, 2012.

[70] S. Debnath, B. Das, P. R. Randive, and K. M. Pandey, "Performance analysis of solar air collector in the climatic condition of North Eastern India," *Energy*, vol. 165, pp. 281–298, 2018.

[71] H. K. Ghritlahre and R. K. Prasad, "Exergetic performance prediction of solar air heater using MLP, GRNN and RBF models of artificial neural network technique," *Journal of Environmental Management*, vol. 223, pp. 566–575, 2018.

[72] K. Taheri, R. Gadow, and A. Killinger, "Exergy analysis as a developed concept of energy efficiency optimized processes: the case of thermal spray processes," *Procedia CIRP*, vol. 17, pp. 511–516, 2014.

[73] S. R. Park, A. K. Pandey, V. Tyagi, and S. K. Tyagi, "Energy and exergy analysis of typical renewable energy systems," *Renewable and Sustainable Energy Reviews*, vol. 30, pp. 105–123, 2014.

[74] S. K. Tyagi, V. V. Tyagi, S. Anand, V. Chandra, and R. C. Diwedi, "First and second law analyses of a typical solar air dryer system: a case study," *International Journal of Sustainable Energy*, vol. 29, no. 1, pp. 8–18, 2010.

[75] A. Kumar, M. Sharma, P. Thakur, V. K. Thakur, S. S. Rahatekar, and R. Kumar, "A review on exergy analysis of solar parabolic collectors," *Solar Energy*, vol. 197, pp. 411–432, 2020.

[76] G. Kalaiarasi, R. Velraj, and M. V. Swami, "Experimental energy and exergy analysis of a flat plate solar air heater with a new design of integrated sensible heat storage," *Energy*, vol. 111, pp. 609–619, 2016.

[77] B. M. Ramani, A. Gupta, and R. Kumar, "Performance of a double pass solar air collector," *Solar Energy*, vol. 84, no. 11, pp. 1929–1937.

[78] F. Kreith and M. B.-P. Grove, *Principles of Heat Transfer (6th uppl.)*, Brooks/Cole Thomson Learning, Pacific Grove, Kalifornien, USA, 2001.

[79] C. E. Bensaci, A. Moummi, F. J. Sanchez de la Flor, E. A. Rodriguez Jara, A. Rincon-Casado, and A. Ruiz-Pardo, "Numerical and experimental study of the heat transfer and hydraulic performance of solar air heaters with different baffle positions," *Renewable Energy*, vol. 155, pp. 1231–1244, 2020.

[80] R. L. Webb and E. R. G. Eckert, "Application of rough surfaces to heat exchanger design," *International Journal of Heat and Mass Transfer*, vol. 15, no. 9, pp. 1647–1658, 1972.

[81] S. K. Sharma and V. R. Kalamkar, "Thermo-hydraulic performance analysis of solar air heaters having artificial roughness-a review," *Renewable and Sustainable Energy Reviews*, vol. 41, pp. 413–435, 2015.

[82] A. Araújo, "Thermo-hydraulic performance of solar air collectors with artificially roughened absorbers: a comparative review of semi-empirical models," *Energies*, vol. 13, no. 14, p. 3536, 2020.

[83] I. Singh and S. Singh, "A review of artificial roughness geometries employed in solar air heaters," *Renewable and Sustainable Energy Reviews*, vol. 92, pp. 405–425, 2018.

[84] A. Kumar and A. Layek, "Thermo-hydraulic performance of roughened solar air heater by design of experiment and metaheuristic approach," *Thermal Science and Engineering Progress*, vol. 10, pp. 92–102, 2019.

[85] A. Kumar, D. K. Rajak, and R. Kumar, "Optimization of packed bed solar air heaters—a thermo-hydraulic approach," *Energy Storage*, vol. 2, no. 2, 2020.

[86] A. Kumar and M.-H. Kim, "Thermal hydraulic performance in a solar air heater channel with multi V-type perforated baffles," *Energies*, vol. 9, no. 7, p. 564, 2016.

[87] V. B. Gawande, A. S. Dhoble, D. B. Zodpe, and S. Chamoli, "Experimental and CFD investigation of convection heat transfer in solar air heater with reverse L-shaped ribs," *Solar Energy*, vol. 131, pp. 275–295, 2016.

[88] R. S. Gill, V. S. Hans, and S. Singh, "Investigations on thermo-hydraulic performance of broken arc rib in a rectangular duct of solar air heater," *International Communications in Heat and Mass Transfer*, vol. 88, pp. 20–27, 2017.

[89] S. Singh, "Performance evaluation of a novel solar air heater with arched absorber plate," *Renewable Energy*, vol. 114, pp. 879–886, 2017.

[90] D. S. Thakur, M. K. Khan, and M. Pathak, "Performance evaluation of solar air heater with novel hyperbolic rib geometry," *Renewable Energy*, vol. 105, pp. 786–797, 2017.

[91] V. B. Gawande, A. S. Dhoble, D. B. Zodpe, and C. Mangrulkar, "A comparative analysis of thermohydraulic performance of a roughened solar air heater using various rib shapes," *Australian Journal of Mechanical Engineering*, vol. 18, no. 3, pp. 331–350, 2018.

[92] A. Kumar and A. Layek, "Thermo-hydraulic performance of solar air heater having twisted rib over the absorber plate," *International Journal of Thermal Sciences*, vol. 133, pp. 181–195, 2018.

[93] M. S. Manjunath, K. V. Karanth, and N. Y. Sharma, "Numerical investigation on heat transfer enhancement of solar air heater using sinusoidal corrugations on absorber plate," *International Journal of Mechanical Sciences*, vol. 138–139, pp. 219–228, 2018.

[94] S. S. Patel and A. Lanjewar, "Experimental analysis for augmentation of heat transfer in multiple discrete V-patterns

combined with staggered ribs solar air heater," *Renewable Energy Focus*, vol. 25, pp. 31–39, 2018.

[95] Y. Menni, A. J. Chamkha, G. Lorenzini, and B. Benyoucef, "Computational fluid dynamics based numerical simulation of thermal and thermo-hydraulic performance of a solar air heater channel having various ribs on absorber plates," *Mathematical Modelling of Engineering Problems*, vol. 6, no. 2, pp. 170–174, 2019.

[96] P. J. Bezbaruah, R. S. Das, and B. K. Sarkar, "Thermo-hydraulic performance augmentation of solar air duct using modified forms of conical vortex generators," *Heat and Mass Transfer*, vol. 55, no. 5, pp. 1387–1403, 2019.

[97] C. Sivakandhan, T. V. Arjunan, and M. M. Matheswaran, "Thermohydraulic performance enhancement of a new hybrid duct solar air heater with inclined rib roughness," *Renewable Energy*, vol. 147, pp. 2345–2357, 2020.

[98] D. J. Dezan, A. D. Rocha, L. O. Salviano, and W. G. Ferreira, "Thermo-hydraulic optimization of a solar air heater duct with non-periodic rows of rectangular winglet pairs," *Solar Energy*, vol. 207, pp. 1172–1190, 2020.

[99] K. Nidhul, S. Kumar, A. K. Yadav, and S. Anish, "Enhanced thermo-hydraulic performance in a V-ribbed triangular duct solar air heater: CFD and exergy analysis," *Energy*, vol. 200, p. 117448, 2020.

[100] A. E. Kabeel, M. H. Hamed, Z. M. Omara, and A. W. Kandeal, "Solar air heaters: design configurations, improvement methods and applications – a detailed review," *Renewable and Sustainable Energy Reviews*, vol. 70, pp. 1189–1206, 2017.

[101] S. Haldorai, S. Gurusamy, and M. Pradhapraj, "A review on thermal energy storage systems in solar air heaters," *International Journal of Energy Research*, vol. 43, no. 12, pp. 6061–6077, 2019.

[102] M. Mofijur, T. Mahlia, A. Silitonga et al., "Phase change materials (PCM) for solar energy usages and storage: an overview," *Energies*, vol. 12, no. 16, p. 3167, 2019.

[103] S. Suman, M. K. Khan, and M. Pathak, "Performance enhancement of solar collectors—a review," *Renewable and Sustainable Energy Reviews*, vol. 49, pp. 192–210, 2015.

[104] A. Kumar and M. H. Kim, "Solar air-heating system with packed-bed energy-storage systems," *Renewable and Sustainable Energy Reviews*, vol. 72, pp. 215–227, 2017.

[105] A. Priyam and P. Chand, "Thermal and thermohydraulic performance of wavy finned absorber solar air heater," *Solar Energy*, vol. 130, pp. 250–259, 2016.

[106] W. Gao, W. Lin, T. Liu, and C. Xia, "Analytical and experimental studies on the thermal performance of cross-corrugated and flat-plate solar air heaters," *Applied Energy*, vol. 84, no. 4, pp. 425–441, 2007.

[107] A. E. Kabeel, M. H. Hamed, Z. M. Omara, and A. W. Kandeal, "Influence of fin height on the performance of a glazed and bladed entrance single-pass solar air heater," *Solar Energy*, vol. 162, pp. 410–419, 2018.

[108] A. M. Lanjewar, J. L. Bhagoria, and M. K. Agrawal, "Review of development of artificial roughness in solar air heater and performance evaluation of different orientations for double arc rib roughness," *Renewable and Sustainable Energy Reviews*, vol. 43, pp. 1214–1223, 2015.

[109] V. Singh Bisht, A. Kumar Patil, and A. Gupta, "Review and performance evaluation of roughened solar air heaters," *Renewable and Sustainable Energy Reviews*, vol. 81, pp. 954–977, 2018.

[110] M. MesgarPour, A. Heydari, and S. Wongwises, "Geometry optimization of double pass solar air heater with helical flow path," *Solar Energy*, vol. 213, pp. 67–80, 2021.

[111] A. Heydari and M. Mesgarpour, "Experimental analysis and numerical modeling of solar air heater with helical flow path," *Solar Energy*, vol. 162, pp. 278–288, 2018.

[112] B. Jia, F. Liu, and D. Wang, "Experimental study on the performance of spiral solar air heater," *Solar Energy*, vol. 182, pp. 16–21, 2019.

[113] P. J. Bezbaruah, R. S. Das, and B. K. Sarkar, "Solar air heater with finned absorber plate and helical flow path: a CFD analysis," *Applied Solar Energy*, vol. 56, no. 1, pp. 35–41, 2020.

[114] I. Singh and S. Vardhan, "Experimental investigation of an evacuated tube collector solar air heater with helical inserts," *Renewable Energy*, vol. 163, pp. 1963–1972, 2021.

[115] A. Saxena, N. Agarwal, and E. Cuce, "Thermal performance evaluation of a solar air heater integrated with helical tubes carrying phase change material," *Journal of Energy Storage*, vol. 30, p. 101406, 2020.

[116] S. Bhattacharyya, M. Pathak, M. Sharifpur, S. Chamoli, and D. R. E. Ewim, "Heat transfer and exergy analysis of solar air heater tube with helical corrugation and perforated circular disc inserts," *Journal of Thermal Analysis and Calorimetry*, pp. 1–6, 2020.

[117] G. Murali, K. R. K. Reddy, M. T. S. Kumar, J. SaiManikanta, and V. N. K. Reddy, "Performance of solar aluminium can air heater using sensible heat storage," *Materials Today: Proceedings*, vol. 21, pp. 169–174, 2020.

[118] S. Vijayan, T. V. Arjunan, A. Kumar, and M. M. Matheswaran, "Experimental and thermal performance investigations on sensible storage based solar air heater," *Journal of Energy Storage*, vol. 31, p. 101620, 2020.

[119] S. Ayyappan, K. Mayilsamy, and V. V. Sreenarayanan, "Performance improvement studies in a solar greenhouse drier using sensible heat storage materials," *Heat and Mass Transfer*, vol. 52, no. 3, pp. 459–467, 2016.

[120] F. S. Javadi, H. S. C. Metselaar, and P. Ganesan, "Performance improvement of solar thermal systems integrated with phase change materials (PCM), a review," *Solar Energy*, vol. 206, pp. 330–352, 2020.

[121] R. Karthikeyan, R. Arul Kumar, P. Manikandan, and A. K. Senthilnathan, "Investigation of solar air heater with phase change materials using packed bed absorber plate," *Materials Today: Proceedings*, 2020.

[122] B. A. SunilRaj and M. Eswaramoorthy, "Experimental study on hybrid natural circulation type solar air heater with paraffin wax based thermal storage," *Materials Today: Proceedings*, vol. 23, pp. 49–52, 2019.

[123] A. K. Raj, M. Srinivas, and S. Jayaraj, "Transient CFD analysis of macro-encapsulated latent heat thermal energy storage containers incorporated within solar air heater," *International Journal of Heat and Mass Transfer*, vol. 156, p. 119896, 2020.

[124] A. Sharma, R. Chauhan, M. Ali Kallioğlu, V. Chinnasamy, and T. Singh, "A review of phase change materials (PCMs) for thermal storage in solar air heating systems," *Materials Today: Proceedings*, 2020.

[125] B. K. Mahmoud, S. I. Ibrahim, K. I. Abass, A. J. Ali, and M. T. Chaichan, "Flat solar air heater collector with phase change materials for domestic purposes in Iraqi climate," *IOP*

Conference Series: Materials Science and Engineering, vol. 928, no. 2, p. 022099, 2020.

[126] Q. A. Jawad, A. M. J. Mahdy, A. H. Khuder, and M. T. Chaichan, "Improve the performance of a solar air heater by adding aluminum chip, paraffin wax, and nano-SiC," *Case Studies in Thermal Engineering*, vol. 19, p. 100622, 2020.

[127] T. K. Abdelkader, Y. Zhang, E. S. Gaballah, S. Wang, Q. Wan, and Q. Fan, "Energy and exergy analysis of a flat-plate solar air heater coated with carbon nanotubes and cupric oxide nanoparticles embedded in black paint," *Journal of Cleaner Production*, vol. 250, p. 119501, 2020.

[128] R. Kumar, S. K. Verma, and V. K. Sharma, "Performance enhancement analysis of triangular solar air heater coated with nanomaterial embedded in black paint," *Materials Today: Proceedings*, vol. 26, pp. 2528–2532, 2019.

[129] P. Dhiman and S. Singh, "Recyclic double pass packed bed solar air heaters," *International Journal of Thermal Sciences*, vol. 87, pp. 215–227, 2015.

[130] S. Singh, "Experimental and numerical investigations of a single and double pass porous serpentine wavy wiremesh packed bed solar air heater," *Renewable Energy*, vol. 145, pp. 1361–1387, 2020.

[131] S. Singh, L. Dhruw, and S. Chander, "Experimental investigation of a double pass converging finned wire mesh packed bed solar air heater," *Journal of Energy Storage*, vol. 21, pp. 713–723, 2019.

[132] C. Dosapati and M. J. K. Mandapati, "Thermal performance of a packed bed double pass solar air heater with a latent heat storage system: an experimental investigation," *World Journal of Engineering*, vol. 17, no. 2, pp. 203–213, 2019.

[133] A. Roy and M. E. Hoque, "Performance analysis of double pass solar air heater with packed bed porous media in Rajshahi," *AIP Conference Proceedings*, vol. 1851, 2017.

[134] V. K. Chouksey and S. P. Sharma, "Investigations on thermal performance characteristics of wire screen packed bed solar air heater," *Solar Energy*, vol. 132, pp. 591–605, 2016.

[135] A. Priyam, P. Chand, and S. P. Sharma, "Energy and exergy analysis of wavy finned absorber solar air heater," *International Journal of Energy Research*, vol. 16, no. 3, pp. 119–130, 2016.

[136] S. Singh and P. Dhiman, "Using an analytical approach to investigate thermal performance of double-flow packed-bed solar air heaters with external recycle," *Journal of Energy Engineering*, vol. 141, no. 3, p. 04014031, 2015.

[137] A. J. Mahmood, L. B. Y. Aldabbagh, and F. Egelioglu, "Investigation of single and double pass solar air heater with transverse fins and a package wire mesh layer," *Energy Conversion and Management*, vol. 89, pp. 599–607, 2015.

[138] R. Kumar and P. Chand, "Performance enhancement of solar air heater using herringbone corrugated fins," *Energy*, vol. 127, pp. 271–279, 2017.

[139] E. A. Handoyo, D. Ichsani, and S. Prabowo, "Numerical studies on the effect of delta-shaped obstacles' spacing on the heat transfer and pressure drop in v-corrugated channel of solar air heater," *Solar Energy*, vol. 131, pp. 47–60, 2016.

[140] A. M. Aboghrara, B. T. H. T. Baharudin, M. A. Alghoul, N. M. Adam, A. A. Hairuddin, and H. A. Hasan, "Performance analysis of solar air heater with jet impingement on corrugated absorber plate," *Case Studies in Thermal Engineering*, vol. 10, pp. 111–120, 2017.

[141] A. E. Kabeel, A. Khalil, S. M. Shalaby, and M. E. Zayed, "Experimental investigation of thermal performance of flat and v-corrugated plate solar air heaters with and without PCM as thermal energy storage," *Energy Conversion and Management*, vol. 113, pp. 264–272, 2016.

[142] S. Darici and A. Kilic, "Comparative study on the performances of solar air collectors with trapezoidal corrugated and flat absorber plates," *Heat and Mass Transfer*, vol. 56, no. 6, pp. 1833–1843, 2020.

[143] W. Lin, H. Ren, and Z. Ma, "Mathematical modelling and experimental investigation of solar air collectors with corrugated absorbers," *Renewable Energy*, vol. 145, pp. 164–179, 2020.

[144] W. Zheng, H. Zhang, S. You, Y. Fu, and X. Zheng, "Thermal performance analysis of a metal corrugated packing solar air collector in cold regions," *Applied Energy*, vol. 203, pp. 938–947, 2017.

[145] S. Singh, B. Singh, V. S. Hans, and R. S. Gill, "CFD (computational fluid dynamics) investigation on Nusselt number and friction factor of solar air heater duct roughened with non-uniform cross-section transverse rib," *Energy*, vol. 84, pp. 509–517, 2015.

[146] I. Singh and S. Singh, "CFD analysis of solar air heater duct having square wave profiled transverse ribs as roughness elements," *Solar Energy*, vol. 162, pp. 442–453, 2018.

[147] P. K. Jain and A. Lanjewar, "Overview of V-rib geometries in solar air heater and performance evaluation of a new V-rib geometry," *Renewable Energy*, vol. 133, pp. 77–90, 2019.

[148] S. Singh Patel and A. Lanjewar, "Experimental and numerical investigation of solar air heater with novel V-rib geometry," *Journal of Energy Storage*, vol. 21, pp. 750–764, 2019.

[149] J. L. Bhagoria, J. S. Saini, and S. C. Solanki, "Heat transfer coefficient and friction factor correlations for rectangular solar air heater duct having transverse wedge shaped rib roughness on the absorber plate," *Renewable Energy*, vol. 25, no. 3, pp. 341–369, 2002.

[150] A. R. Jaurker, J. S. Saini, and B. K. Gandhi, "Heat transfer and friction characteristics of rectangular solar air heater duct using rib-grooved artificial roughness," *Solar Energy*, vol. 80, no. 8, pp. 895–907, 2006.

[151] S. V. Karmare and A. N. Tikekar, "Analysis of fluid flow and heat transfer in a rib grit roughened surface solar air heater using CFD," *Solar Energy*, vol. 84, no. 3, pp. 409–417, 2010.

[152] S. V. Karmare and A. N. Tikekar, "Experimental investigation of optimum thermohydraulic performance of solar air heaters with metal rib grits roughness," *Solar Energy*, vol. 83, no. 1, pp. 6–13, 2009.

[153] S. V. Karmare and A. N. Tikekar, "Heat transfer and friction factor correlation for artificially roughened duct with metal grit ribs," *International Journal of Heat and Mass Transfer*, vol. 50, no. 21–22, pp. 4342–4351, 2007.

[154] H. K. Ghritlahre, P. K. Sahu, and S. Chand, "Thermal performance and heat transfer analysis of arc shaped roughened solar air heater - an experimental study," *Solar Energy*, vol. 199, pp. 173–182, 2020.

[155] N. Kumar Pandey, V. Kumar Bajpai, and S. Yadav, "Influence of number of gaps created in a arc shaped roughened absorber plate used in solar air-heaters," *IOP Conference Series: Materials Science and Engineering*, vol. 691, no. 1, 2019.

[156] H. K. Ghritlahre and R. K. Prasad, "Prediction of exergetic efficiency of arc shaped wire roughened solar air heater using ANN model," *International Journal of Heat and Technology*, vol. 36, no. 3, pp. 1107–1115, 2018.

[157] M. K. Sahu and R. K. Prasad, "Investigation on optimal thermohydraulic performance of a solar air heater having arc shaped wire rib roughness on absorber plate," *Int. J. Thermodyn*, vol. 19, no. 4, pp. 214–224, 2016.

[158] P. T. Saravanakumar, D. Somasundaram, and M. M. Matheswaran, "Thermal and thermo-hydraulic analysis of arc shaped rib roughened solar air heater integrated with fins and baffles," *Solar Energy*, vol. 180, pp. 360–371, 2019.

[159] P. T. Saravanakumar, D. Somasundaram, and M. M. Matheswaran, "Exergetic investigation and optimization of arc shaped rib roughened solar air heater integrated with fins and baffles," *Applied Thermal Engineering*, vol. 175, p. 115316, 2020.

[160] K. D. Yadav and R. K. Prasad, "Performance analysis of parallel flow flat plate solar air heater having arc shaped wire roughened absorber plate," *Renew Energy Focus*, vol. 32, pp. 23–44, 2020.

[161] S. K. Jain, G. D. Agrawal, and M. Varshney, "CFD simulation of artificially roughened solar air heater using discrete W-shaped ribs," *Proc. 2017 IEEE Int. Conf. Technol. Adv. Power Energy Explor. Energy Solut. an Intell. Power Grid, TAP Energy 2017*, pp. , 20181–6, 2018.

[162] D. Jin, M. Zhang, P. Wang, and S. Xu, "Numerical investigation of heat transfer and fluid flow in a solar air heater duct with multi V-shaped ribs on the absorber plate," *Energy*, vol. 89, pp. 178–190, 2015.

[163] A. Kumar and M.-H. Kim, "CFD analysis on the thermal hydraulic performance of an SAH duct with multi V-shape roughened ribs," *Energies*, vol. 9, no. 6, p. 415, 2016.

[164] S. S. Patel and A. Lanjewar, "Exergy based analysis of solar air heater duct with W-shaped rib roughness on the absorber plate," *Arch. Thermodyn.*, vol. 40, no. 4, pp. 21–48, 2019.

[165] S. Thakur and N. S. Thakur, "Investigational analysis of roughened solar air heater channel having W-shaped ribs with symmetrical gaps along with staggered ribs," *Energy Sources, Part A: Recovery, Utilization, and Environmental Effects*, pp. 1–16, 2019.

[166] S. Singh, S. Chander, and J. S. Saini, "Exergy based analysis of solar air heater having discrete V-down rib roughness on absorber plate," *Energy*, vol. 37, no. 1, pp. 749–758, 2012.

[167] A. K. Patil, J. S. Saini, and K. Kumar, "Effect of gap position in broken V-rib roughness combined with staggered rib on thermohydraulic performance of solar air heater," *Green*, vol. 1, no. 5–6, pp. 329–338, 2011.

[168] A. K. Patil, J. S. Saini, and K. Kumar, "Heat transfer and friction characteristics of solar air heater duct roughened by broken V-shape ribs combined with staggered rib piece," *Journal of Renewable and Sustainable Energy*, vol. 4, no. 1, pp. 604–610, 2012.

[169] M. Sethi and N. S. T. Varun, "Correlations for solar air heater duct with dimpled shape roughness elements on absorber plate," *Solar Energy*, vol. 86, no. 9, pp. 2852–2861, 2012.

[170] S. Yadav, M. Kaushal, Varun, and Siddhartha, "Nusselt number and friction factor correlations for solar air heater duct having protrusions as roughness elements on absorber plate," *Experimental Thermal and Fluid Science*, vol. 44, pp. 34–41, 2013.

[171] A. Kumar, R. P. Saini, and J. S. Saini, "Development of correlations for Nusselt number and friction factor for solar air heater with roughened duct having multi v-shaped with gap rib as artificial roughness," *Renewable Energy*, vol. 58, pp. 151–163, 2013.

[172] A. P. Singh, Varun, and Siddhartha, "Heat transfer and friction factor correlations for multiple arc shape roughness elements on the absorber plate used in solar air heaters," *Experimental Thermal and Fluid Science*, vol. 54, pp. 117–126, 2014.

[173] R. Maithani and J. S. Saini, "Heat transfer and fluid flow behaviour of a rectangular duct roughened with V-ribs with symmetrical gaps," *International Journal of Ambient Energy*, vol. 38, no. 4, pp. 347–355, 2017.

[174] R. Maithani and J. S. Saini, "Performance evaluation of solar air heater having V-ribs with symmetrical gaps in a rectangular duct of solar air heater," *International Journal of Ambient Energy*, vol. 38, no. 4, pp. 400–410, 2017.

[175] R. Maithani and J. S. Saini, "Heat transfer and friction factor correlations for a solar air heater duct roughened artificially with V-ribs with symmetrical gaps," *Experimental Thermal and Fluid Science*, vol. 70, pp. 220–227, 2016.

[176] N. S. Deo, S. Chander, and J. S. Saini, "Performance analysis of solar air heater duct roughened with multigap V-down ribs combined with staggered ribs," *Renewable Energy*, vol. 91, pp. 484–500, 2016.

[177] N. K. Pandey and V. K. B. Varun, "Experimental investigation of heat transfer augmentation using multiple arcs with gap on absorber plate of solar air heater," *Solar Energy*, vol. 134, pp. 314–326, 2016.

[178] V. S. Hans, R. S. Gill, and S. Singh, "Heat transfer and friction factor correlations for a solar air heater duct roughened artificially with broken arc ribs," *Experimental Thermal and Fluid Science*, vol. 80, pp. 77–89, 2017.

[179] R. S. Gill, V. S. Hans, J. S. Saini, and S. Singh, "Investigation on performance enhancement due to staggered piece in a broken arc rib roughened solar air heater duct," *Renewable Energy*, vol. 104, pp. 148–162, 2017.

[180] K. Kumar, D. R. Prajapati, and S. Samir, "Heat transfer and friction factor correlations development for solar air heater duct artificially roughened with 'S' shape ribs," *Experimental Thermal and Fluid Science*, vol. 82, pp. 249–261, 2017.

[181] A. Kumar, R. Kumar, R. Maithani et al., "Correlation development for Nusselt number and friction factor of a multiple type V-pattern dimpled obstacles solar air passage," *Renewable Energy*, vol. 109, pp. 461–479, 2017.

[182] D. S. Thakur, M. K. Khan, and M. Pathak, "Solar air heater with hyperbolic ribs: 3D simulation with experimental validation," *Renewable Energy*, vol. 113, pp. 357–368, 2017.

[183] F. Menasria, M. Zedairia, and A. Moummi, "Numerical study of thermohydraulic performance of solar air heater duct equipped with novel continuous rectangular baffles with high aspect ratio," *Energy*, vol. 133, pp. 593–608, 2017.

[184] D. Jin, J. Zuo, S. Quan, S. Xu, and H. Gao, "Thermohydraulic performance of solar air heater with staggered multiple V-shaped ribs on the absorber plate," *Energy*, vol. 127, pp. 68–77, 2017.

[185] S. K. Sharma and V. R. Kalamkar, "Experimental and numerical investigation of forced convective heat transfer in solar air heater with thin ribs," *Solar Energy*, vol. 147, pp. 277–291, 2017.

[186] S. Mirjalili, J. Song Dong, and A. Lewis, *Nature-Inspired Optimizers*, vol. 811, Springer International Publishing, 2020.

[187] E. Koutroulis, D. Kolokotsa, A. Potirakis, and K. Kalaitzakis, "Methodology for optimal sizing of stand-alone photovoltaic/wind-generator systems using genetic algorithms," *Solar Energy*, vol. 80, no. 9, pp. 1072–1088, 2006.

[188] S. A. Kalogirou, "Optimization of solar systems using artificial neural-networks and genetic algorithms," *Applied Energy*, vol. 77, no. 4, pp. 383–405, 2004.

[189] M. Loomans and H. Visser, "Application of the genetic algorithm for optimisation of large solar hot water systems," *Solar Energy*, vol. 72, no. 5, pp. 427–439, 2002.

[190] S. Nesmachnow, "An overview of metaheuristics: accurate and efficient methods for optimisation," *International Journal of Metaheuristics*, vol. 3, no. 4, 2014.

[191] U. Khaled, A. M. Eltamaly, and A. Beroual, "Optimal power flow using particle swarm optimization of renewable hybrid distributed generation," *Energies*, vol. 10, no. 7, 2017.

[192] J. C. Bansal, *Evolutionary and Swarm Intelligence Algorithms*, vol. 779, Springer International Publishing, 2019.

[193] K. L. Du and M. N. S. Swamy, *Search and Optimization by Metaheuristics: Techniques and Algorithms Inspired by Nature*, Search Optim. by Metaheuristics Tech. Algorithms Inspired by Nat., 2016.

[194] C. P. Mohanty, A. K. Behura, M. R. Singh et al., "Parametric performance optimization of three sides roughened solar air heater," *Energy Sources, Part A: Recovery, Utilization, and Environmental Effects*, pp. 1–21, 2020.

[195] R. V. Rao, V. J. Savsani, and D. P. Vakharia, "Teaching-learning-based optimization: a novel method for constrained mechanical design optimization problems," *Computer-Aided Design*, vol. 43, no. 3, pp. 303–315, 2011.

[196] R. V. Rao, V. J. Savsani, and J. Balic, "Teaching-learning-based optimization algorithm for unconstrained and constrained real-parameter optimization problems," *Engineering Optimization*, vol. 44, no. 12, pp. 1447–1462, 2012.

[197] R. V. Rao, V. J. Savsani, and D. P. Vakharia, "Teaching-learning-based optimization: an optimization method for continuous non-linear large scale problems," *Information Sciences*, vol. 183, no. 1, pp. 1–15, 2012.

[198] R. V. Rao, "Teaching-learning-based optimization algorithm," in *Teaching Learning Based Optimization Algorithm*, pp. 9–39, Springer International Publishing, 2016.

[199] R. V. Rao, "Review of applications of TLBO algorithm and a tutorial for beginners to solve the unconstrained and constrained optimization problems," *Decision Science Letters*, vol. 5, no. 1, pp. 1–30, 2016.

[200] R. V. Rao, "Design of a smooth flat plate solar air heater using TLBO and ETLBO algorithms," in *Teaching Learning Based Optimization Algorithm*, pp. 137–161, Springer International Publishing, 2016.

[201] R. V. Rao and V. Patel, "An elitist teaching-learning-based optimization algorithm for solving complex constrained optimization problems," *international journal of industrial engineering computations*, vol. 3, no. 4, pp. 535–560, 2012.

[202] Varun and Siddhartha, "Thermal performance optimization of a flat plate solar air heater using genetic algorithm," *Applied Energy*, vol. 87, no. 5, pp. 1793–1799, 2010.

[203] A. Ş. Şahin, "Optimization of solar air collector using genetic algorithm and artificial bee colony algorithm," *Heat and Mass Transfer*, vol. 48, no. 11, pp. 1921–1928, 2012.

[204] A. Gholami, Y. Ajabshirchi, and S. F. Ranjbar, "Thermo-economic optimization of solar air heaters with arcuate-shaped obstacles," *Journal of Thermal Analysis and Calorimetry*, vol. 138, no. 2, pp. 1395–1403, 2019.

[205] D. Karaboga, B. Gorkemli, C. Ozturk, and N. Karaboga, "A comprehensive survey: artificial bee colony (ABC) algorithm and applications," *Artificial Intelligence Review*, vol. 42, no. 1, pp. 21–57, 2014.

[206] M. S. Kiran and O. Findik, "A directed artificial bee colony algorithm," *Applied Soft Computing*, vol. 26, pp. 454–462, 2015.

[207] M. K. Das, K. Kumar, T. K. Barman, and P. Sahoo, "Application of artificial bee colony algorithm for optimization of MRR and surface roughness in EDM of EN31 tool steel," *Procedia Materials Science*, vol. 6, pp. 741–751, 2014.

[208] S. Kirkpatrick, C. D. Gelatt, and M. P. Vecchi, "Optimization by simulated annealing," *Science*, vol. 220, no. 4598, pp. 671–680, 1983.

[209] A. M. Zain, H. Haron, and S. Sharif, "Simulated annealing to estimate the optimal cutting conditions for minimizing surface roughness in end milling Ti-6Al-4V," *Machining Science and Technology*, vol. 14, no. 1, pp. 43–62, 2010.

[210] S. R. C. Siddhartha and N. S. Varun, "Thermal performance optimization of smooth flat plate solar air heater (SFPSAH) using simulated annealing: evaluation and comparisons," in *2011 International Conference & Utility Exhibition on Power and Energy Systems: Issues and Prospects for Asia (ICUE)*, pp. 1–5, 2012.

[211] S. Shafiee and E. Topal, "When will fossil fuel reserves be diminished?," *Energy Policy*, vol. 37, no. 1, pp. 181–189, 2009.

[212] J. H. Liang and C. H. Lee, "A modification artificial bee colony algorithm for optimization problems," *Mathematical Problems in Engineering*, vol. 2015, 2015.

[213] S. Kessentini and D. Barchiesi, "Particle swarm optimization with adaptive inertia weight," *International Journal of Machine Learning and Computing*, vol. 5, no. 5, pp. 368–373, 2015.

[214] S. S. Ilango, S. Vimal, M. Kaliappan, and P. Subbulakshmi, "Optimization using artificial bee colony based clustering approach for big data," *Cluster Computing*, vol. 22, pp. 12169–12177, 2019.

[215] Z. Wu, W. Fu, R. Xue, and W. Wang, "A novel global path planning method for mobile robots based on teaching-learning-based optimization," *Information*, vol. 7, no. 3, 2016.

[216] T. Zhu and J. Zhang, "A numerical study on performance optimization of a micro-heat pipe arrays-based solar air heater," *Energy*, vol. 215, p. 119047, 2021.

[217] A. Benhamza, A. Boubekri, A. Atia et al., "Multi-objective design optimization of solar air heater for food drying based on energy, exergy and improvement potential," *Renewable Energy*, vol. 169, 2021.

[218] V. S. Korpale, S. P. Deshmukh, C. S. Mathpati, and V. H. Dalvi, "Numerical simulations and optimization of solar air heaters," *Applied Thermal Engineering*, vol. 180, 2020.

[219] S. F. Ali and D. Rakshit, "Utilising passive design strategies for analysing thermal comfort levels inside an office room using PMV-PPD models," in *Solar Energy*, Energy, Environment, and Sustainability, H. Tyagi, P. Chakraborty, S. Powar, and A. Agarwal, Eds., pp. 35–57, Springer, Singapore, 2020.

[220] P. J. Bezbaruah, R. S. Das, and B. K. Sarkar, "Overall performance analysis and GRA optimization of solar air heater with

truncated half conical vortex generators," *Solar Energy*, vol. 196, pp. 637–652, 2020.

[221] H. Xiao, J. Wang, Z. Liu, and W. Liu, "Turbulent heat transfer optimization for solar air heater with variation method based on exergy destruction minimization principle," *International Journal of Heat and Mass Transfer*, vol. 136, pp. 1096–1105, 2019.

[222] B. S. Qader, E. E. Supeni, M. K. A. Ariffin, and A. R. A. Talib, "RSM approach for modeling and optimization of designing parameters for inclined fins of solar air heater," *Renewable Energy*, vol. 136, pp. 48–68, 2019.

[223] R. Kumar, V. Goel, P. Singh, A. Saxena, A. S. Kashyap, and A. Rai, "Performance evaluation and optimization of solar assisted air heater with discrete multiple arc shaped ribs," *Journal of Energy Storage*, vol. 26, 2019.

[224] S. Debnath, J. Reddy, and J. Das, "Modeling and optimization of flat plate solar air collectors: an integrated fuzzy method," *Journal of Renewable and Sustainable Energy*, vol. 11, no. 4, 2019.